



UNIVERSITAT
POLITÈCNICA
DE VALÈNCIA



Departamento de Sistemas Informáticos y Computación
Universitat Politècnica de València

**DESIGN AND IMPLEMENTATION OF AN
ATRIAL FIBRILLATION DETECTOR BASED
ON NEURAL NETWORKS**

Master Thesis

**Master's Degree in Artificial Intelligence, Pattern
Recognition and Digital Imaging**

Author: Xavier Ibáñez Català

Tutor: Roberto Paredes Palacios

2014-2015



Resumen

La fibrilación auricular (FA) es la arritmia sostenida más frecuente en la población, aumentando su prevalencia con la edad de los pacientes. La sintomatología de la FA reduce considerablemente la calidad de vida. No obstante, la mayor causa de morbimortalidad asociada a la FA es consecuencia del riesgo aumentado de sufrir un accidente cerebrovascular por un trombo de génesis cardíaca. Es por ello que existe un gran interés clínico en el diagnóstico precoz, tratamiento y control de los pacientes con FA.

Este Trabajo Fin de Máster tiene como objetivo el diseño y desarrollo de un detector de FA que sólo utilice la información contenida en los intervalos RR de un segmento de 30 segundos de electrocardiograma. Para ello se emplean redes neuronales y se exploran diferentes técnicas para mejorar sus capacidades de aprendizaje. El detector desarrollado se integra en una aplicación comercial de procesamiento de señal electrocardiográfica de larga duración. Tras la integración, el detector es posteriormente testado según los estándares de aplicación en este ámbito, demostrándose su eficacia.

Palabras clave: ECG, electrocardiografía ambulatoria; fibrilación auricular, detección basada en RR, redes neuronales.

Abstract

Atrial fibrillation (AF) is the most common sustained arrhythmia, increasing its prevalence with the age of the patients. The symptoms of AF considerably reduce the quality of life. However, the most important cause of morbid-mortality associated to AF is consequence of an augmented risk of suffering a stroke as a result of a cardiogenic thrombus. Because of this, clinical community is very interested in an early diagnosis, treatment and control of the patients with AF.

The objective of this Master Thesis is to design and develop an AF detector which only uses the information contained in the inter-beat interval sequence of an electrocardiogram segment of 30 seconds. To achieve this goal, artificial neural networks are employed and several approaches to improve their learning capabilities are explored. The developed detector is integrated in a commercial software solution to analyze long-term electrocardiograms. After the integration, the detector is tested according to the standards applying to this sector, demonstrating its effectiveness.

Keywords: ECG, ambulatory electrocardiography, atrial fibrillation, RR-based detection, neural networks.





Abbreviations

AF: atrial fibrillation.

AFDB: MIT-BIH Atrial Fibrillation Database.

ANN: artificial neural networks.

AUC: area under the curve ROC.

AV: atrio-ventricular.

BIH: Beth Israel Hospital.

ECG: electrocardiogram.

ELR: event loop recorder.

FDA: Food and Drug Administration.

FM: frequency modulation.

HMM: hidden Markov model.

IEC: International Electrotechnical Commission.

ILR: implantable loop recorder.

KS: Kolmogorov-Smirnov.

LTAfDB: MIT-BIH Long Term Atrial Fibrillation Database.

MCT: mobile cardiac telemetry.

MIT: Massachusetts Institute of Technology.

MITDB: MIT-BIH Arrhythmia Database.

MLP: multilayer perceptron.

NSRDB: MIT-BIH Normal Sinus Rhythm Database.

NSRDB_RR: Normal Sinus Rhythm RR Interval Database.

ReLU: rectified linear unit.

SA: sinoatrial.

SME: small and medium-sized enterprise.

VF: ventricular fibrillation.





Table of contents

1. INTRODUCTION	9
2. CLINICAL BACKGROUND	11
The Heart.....	11
Anatomy and Physiology.....	11
Electrophysiology.....	13
Electrocardiography.....	16
Atrial Fibrillation.....	18
Epidemiology and Related Pathologies.....	18
Symptoms and Diagnosis.....	19
3. TECHNICAL BACKGROUND AND STATE OF THE ART	21
Ambulatory ECG Monitoring.....	21
Traditional Holter Test.....	21
Long-Term Cardiac Monitoring.....	22
Atrial Fibrillation Detection.....	29
Evaluation of AF detectors.....	30
Academic Solutions.....	31
Industrial Solutions.....	36
Performance Goals.....	39
4. METHODS	41
Artificial Neural Networks.....	41
Backpropagation.....	43
Output Units for Classification.....	44
Approaches to Improve Learning.....	45
Momentum.....	45
Learning Rate Scaling.....	45
Rectified Linear Unit.....	46
Max-norm regularization.....	47
Dropout.....	48
Toolbox.....	49



5. EXPERIMENTS	51
Database	51
Feature Extraction.....	52
Developing the Classifier.....	53
Common Parameter Tuning.....	53
Defining Histogram Bin Size.....	54
Adding AFDB to the training dataset.....	55
ANN with Dropout	55
ANN with Dropout and ReLU	56
Apply max-norm regularization.....	56
Conclusion.....	56
Hold Out: Results on Test Dataset	57
6. COMMERCIAL PRODUCT DEVELOPMENT	59
Prototype	59
Integration.....	59
7. CONCLUSIONS	61
8. REFERENCES	63
A. ANNEX: BIN SIZE EXPLORATION	67
B. ANNEX: TRAINING WITH AFDB	71
C. ANNEX: ANN WITH DROPOUT	73



1. Introduction

Atrial fibrillation (AF) is the most common sustained arrhythmia, affecting 1–2% of the population. It is a fast arrhythmia characterized by the set up of recurrent, multiple and uncoordinated electrical waves in the atria that excite the atrial myocardium in a totally disorganized way. As a result, atrial contraction is inexistent and ventricular beats are fast and arrhythmic. Patients with AF suffer from different symptoms, such as palpitations, fatigue, faintness or shortness of breath, among others, which considerably reduce their quality of life.

Moreover, as atrial beat is inexistent during AF, blood flows passively to the ventricles, which can generate regions inside the atrium where blood hardly moves. This may cause the blood to coagulate, which can produce stroke and other thromboembolic events. In fact, AF is associated with a 5-fold risk of stroke and an augmented morbi-mortality of stroke patients with AF, compared with those without AF.

AF episodes can self-terminate and the triggering situations of a new episode are not easily predictable. Thus, only an opportunistic ECG could find the arrhythmia. Moreover, assessment of the AF burden is important to decide the treatment or to evaluate the effectiveness of a therapy. It has been estimated that 7 day continuous ECG monitoring may document the arrhythmia in approximately 70% of AF patients. To process these long-term ECG signals, either real-time or offline, AF detection algorithms are needed.

The main goal of this Master Thesis is to develop a classifier able to distinguish between AF and non-AF rhythms using the information contained in the inter-beat interval sequence of an ECG segment of 30 seconds. Thus, every detected beat should be considered and no morphology assessment should be needed in order to eliminate ectopic beats that can be confused with AF rhythm. This way, the classifier could be integrated in any ECG analysis system that performs beat detection, such as implantable or external cardiac monitors or offline analysis platforms as holter analysis software.

This development pursues to achieve better performance than SEEQ, an ECG monitoring patch developed and distributed by Medtronic. This product is, to our concern, the only product that publishes its AF performance results on public standard



databases as disclosed in IEC 60601-2-47, which is the standard that applies for ambulatory electrocardiographs. Thus, the objective is to overcome a sensitivity of 90% and a positive predictivity of 85% on MIT-BIH Arrhythmia Database, the public database specified by the standard.

As a secondary objective, the classification system should be integrated in a software solution to analyze long-term ECG recordings developed by Nuubo, a Spanish company focused on ambulatory electrocardiography based on e-textiles which has developed the first textile holter in the market.

To achieve these goals, artificial neural networks (ANN) will be used. Different approaches to improve the learning capabilities of ANN will be explored, such as employing rectified linear units (ReLU) in the hidden layers or using dropout mechanism, which temporally disables random neurons during training time to improve generalization.



2. Clinical Background

The Heart

Anatomy and Physiology

The heart is one of the body muscular viscera that, together with the blood and the vessels, form the circulatory system. It is responsible for pumping blood allowing it to circulate and carry oxygen and all necessary nutrients to each cell in the body (see Figure 1).

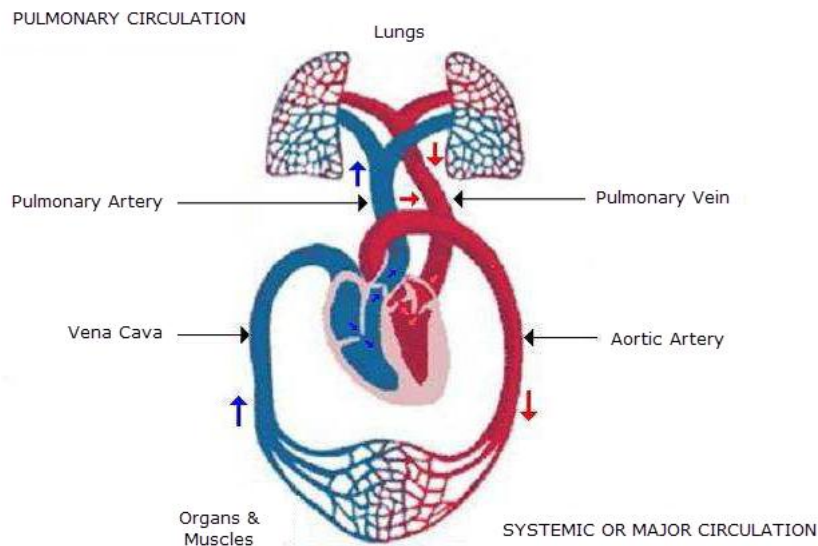


Figure 1. Circulatory system. In the upper part, *pulmonary circulation* is shown, formed by pulmonary artery, lungs and pulmonary vein. This circuit is in charge of oxygenate the blood. In the lower part, *systemic circulation* is shown, formed by aortic artery, all organs and muscles in the body and cava vein. Its function is to carry nutrients and oxygen to all cells in the body, while removing any metabolic residue.

The human heart is divided into four chambers: the two upper chambers are called atria and the two lower ventricles (see Figure 2). The heart is divided by a partition wall, called atrial septum in the upper part and interventricular septum in the lower part, so chambers are only communicated in pairs, right atrium with right ventricle and left atrium with left ventricle. Thus, it is common to speak of the right heart, responsible for receiving blood with CO_2 (blue in Figure 1) and pumping it to the lungs, and of the left heart, responsible for receiving oxygenated blood from the lungs



(red) and pumping it to other body organs. Atria receive blood from veins and pump it to ventricles, while ventricles pump blood to arterial vessels.

Several valves avoid the blood flowing backwards, both between atria and ventricles (tricuspid valve on the right heart and mitral valve on the left heart) and in the beginning of the arterial vessels (pulmonary valve on the right, aortic valve on the left) (see Figure 2). [1]

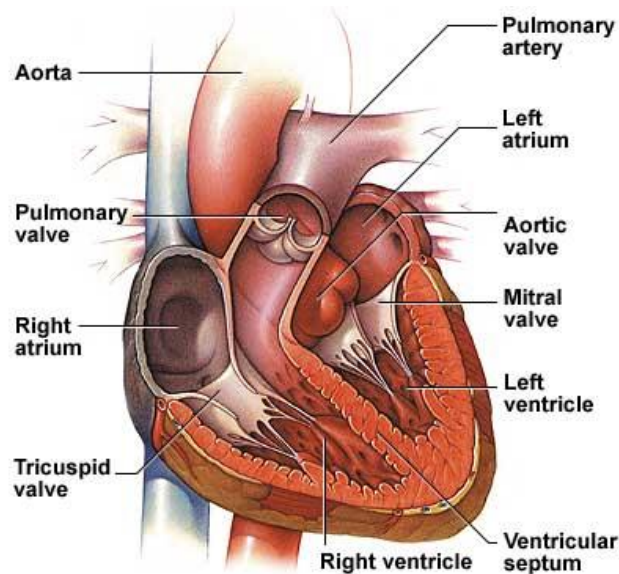


Figure 2. Anatomy of the heart. All four chambers can be distinguished. To avoid the blood flowing backwards, atria and ventricles are separated by tricuspid valve (right heart) and mitral valve (left heart), and also pulmonary valve (right heart) and aortic valve (left heart) can be found between ventricles and arteries.

As it was said before, the heart is a pump which propels the blood through the vascular circuit to every cell in the body, in order to deliver them nutrients and oxygen and also to remove all residues produced in the regular activity of the cells. The mechanical activity of the heart is divided into two phases: diastole and systole.

The cardiac cycle begins with the diastolic stage. In this phase, the atrioventricular valves open, allowing the blood to flow into the ventricles due to the pressure difference between these and the atria. Once the ventricles are nearly full, the flow of blood to them slows in a stage called diastasis. Diastole ends with the atrial cardiac systole, when the atria contraction pumps the blood, which still remains in them, through to the ventricles, allowing a 30% increase of blood volume in the ventricles.

The second phase of the cardiac cycle is the systole. In a first stage an isometric contraction of the ventricles takes place, in which no volume variation occurs, but pressure rises, causing the atrioventricular valve to close. When the intraventricular pressure exceeds the pressure in the artery (aorta or pulmonary, as appropriate) the arterial valves open. At this moment the emptying stage starts, which lasts for about three quarters of the systolic duration. The blood flows from ventricles into arteries until an isometric relaxation of the ventricular fibers occurs. Consequently, the interventricular pressure drops, causing the closure of the arterial valve and the subsequent opening of the atrioventricular valves and thus ending the cycle (see Figure 3) [1].

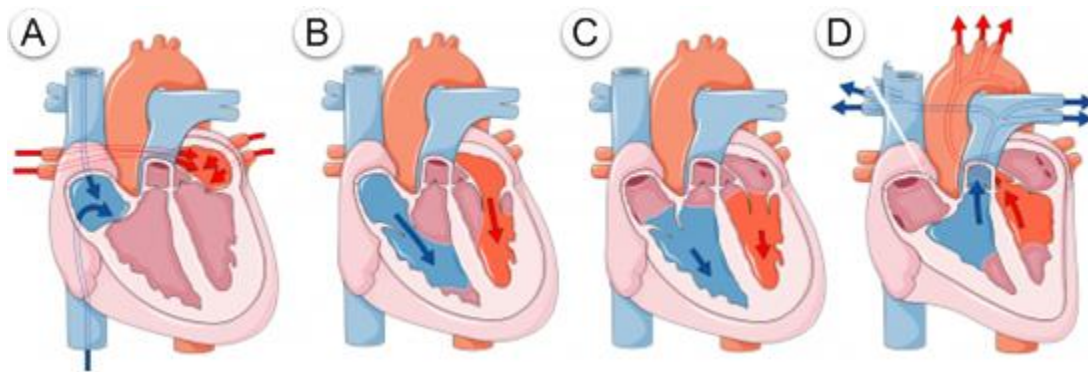


Figure 3. Cardiac cycle. A) Tricuspid and mitral valves are closed because pressure in the ventricle is higher than in the atrium. B) When atrial pressure is higher than ventricular one tricuspid and mitral valves open. C) Atrial contraction helps to fill the ventricles, allowing a 30% increase of its volume. D) Ventricular contraction raises the pressure, opening of arterial and pulmonary valves and pumping the blood to the rest of the body.

Electrophysiology

Synchronized contraction of the muscular heart fibers is needed to guarantee an efficient cardiac pumping. Here below, the underlying electrical activity, which is responsible for the cardiac synchronism and the effective pumping, is described, starting with the micro level, the cell, and going on with the macro level, the specialized electric structures and the cardiac activation sequence.

Cellular electrical activity: the action potential

Cellular membrane is a layer of lipid molecules that almost perfectly isolates the extracellular and intracellular media. Both media are aqueous dissolutions of a variety of solutes such as proteins, glucose and ions. However, ionic concentrations of intracellular and extracellular media are different. This causes a potential difference between the interior of the cell and its exterior. This potential difference is called



resting potential and, in cardiac cells, has a value of approximately -90 mV (being the extracellular medium the reference).

Furthermore, some cells, including cardiomyocytes and neurons, are excitable, that is, they are capable of autonomously increase their potential during a short period of time as a consequence of an external stimulus, generating what is known as action potential. In muscular cells, and thus in cardiomyocytes, contraction is closely linked to the action potential, which has three stages (see Figure 4):

- **Depolarization:** when a cell receives a stimulus that exceeds a certain threshold, a rapid rise of the membrane potential is triggered. This phase is due to a rapid influx of positive charges in the cell (mostly Na^+), and can reach values of around 25 mV.
- **Plateau:** the entrance of Na^+ stops, but then another cation, Ca^{2+} , starts entering into the cell, while K^+ leaves it. At this stage, the electrical charge flow is almost zero, so the membrane potential remains nearly constant. The mechanical contraction of cardiomyocyte occurs during this stage.
- **Repolarization:** at the end of the plateau stages, the Ca^{2+} inflow becomes slower and disappears, but the exit of K^+ is maintained, so that cell potential decreases up to the resting value. When the resting value is restored, different ionic pumping mechanisms are activated to restore the ionic balance in the cell.

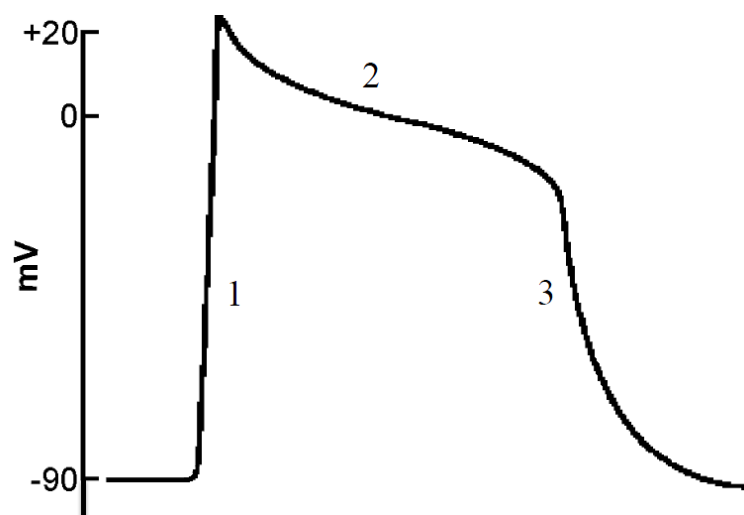


Figure 4. Cardiomyocyte action potential. Three stages can be distinguished: (1) depolarization, (2) Plateau and (3) Repolarization.

As said above, an external stimulus is needed to trigger a potential action (with the exception of some autotriggered cells, as it will be discussed in a next section). A stimulus can be activated in a laboratory by injecting current into the cell with a special

electrode, but in the natural state the stimulus that triggers the action potential of a cardiac cell comes from an adjacent cell. Cardiomyocytes are connected to their neighbors by the so-called intercalated disks, which contain special channels (known as gap junctions) that allow the exchange of ions between cells. Thus, when a cardiac cell is depolarized, it stimulates the depolarization of its neighbors, spreading the electrical stimulus across the myocardium in a short time, allowing this way a synchronous contraction of the cardiac muscle [2].

Propagation of the electric stimulus: the cardiac conduction system

However, in physiological situations the electrical stimulus that triggers cardiac contraction is not originated in the myocardium, but in a particular structure consisting of autoexcitable cells which constitute the heart natural pacemaker. This structure is located at the top wall of the right atrium and is called sinus or sinoatrial node (SA node). A stimulus spreads throughout the atria along Bachmann's bundle (to the left atrium) and along internodal atrial pathways to reach the atrioventricular node (AV node), which is located at the bottom of the right atrium. Atria and ventricles are electrically isolated in their entire contact surface and AV node constitutes the only physiological communication path between them. In AV node the electric signal is delayed, due to its slower conduction velocity. This delay allows the ventricles to fill with blood before the stimulus continues and ventricles contract. After passing the AV node, the stimulus goes through the Hiss bundle, which divides into two branches located within the interventricular septum. The Hiss bundle branches divide into multiple fibers (called Purkinje fibers) with high conduction velocity helping this way, the rapid spreading of the the stimulus throughout the entire ventricle, allowing, then, a synchronized ventricular contraction. The contraction starts in the septum and the lower part of the heart (called apex) and spreads to the upper part of the ventricles [1]. Cardiac conduction system and all its different structures can be seen in Figure 5.

Moreover, it is important to note the absence of back-propagations of the electrical stimulus in a healthy heart. This is because cells are not able to generate or propagate an action potential during a while after finishing a precedent action potential, which is known as refractory period. This property allows stimuli to expire after spreading throughout the whole myocardium, avoiding the creation of re-entry circuits that generate arrhythmias. The existence of arrhythmias is a pathological condition that may develop serious and even fatal consequences.



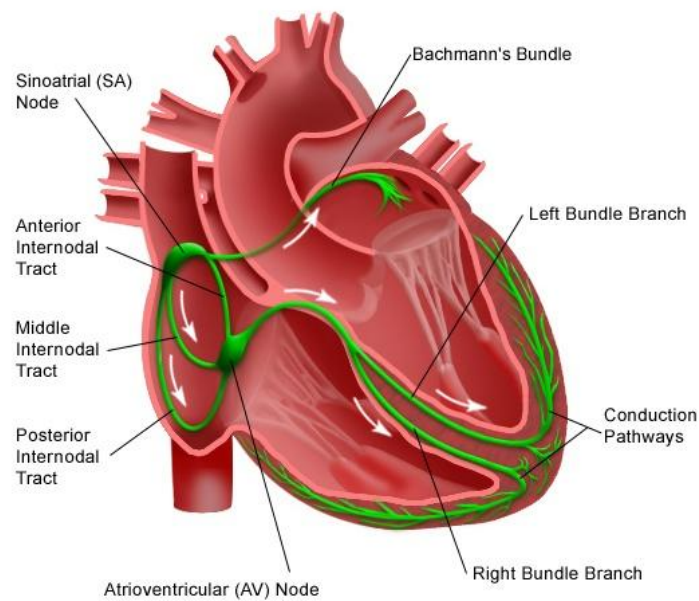


Figure 5. Cardiac conduction system. Electrical stimulus is originated in SA node, and propagated throughout the atrium along Bachmann's bundle and internodal tracts. When reaching AV node, the stimulus is delayed and then propagated through the Hiss bundle to activate the ventricles in a down-top sequence.

Electrocardiography

Corporal fluids and organs surrounding the heart inside the chest are good electric conductors, so depolarization waves spreading throughout the myocardium generate electrical current flows across the chest. These current flows generate electrical potential differences that can be measured on the body surface. The recording of the heart electrical activity by using electrodes placed on a patient's body is called electrocardiography, and the voltage versus time signal resulting from this process is referred to as an electrocardiogram (ECG). Electrical cardiac activity is a 3D process, so different electrode locations will generate different points of view of the cardiac activity. Each different point of view is known as a cardiac lead.

As it has been explained before, in a healthy heart, depolarization wave has an ordered progression: starting in the SA node, spreading throughout the atrium, suffering a delay in the AV node, to pass right afterwards to the ventricles through the Hiss bundle, contracting the ventricular myocardium in an ordered sequence: septum first, and then ventricles are depolarized from down to top. This activation sequence has its reflection on the ECG, producing, for each heartbeat, the characteristic waves known as P-QRS-T. As it can be seen in Figure 6, each wave stands for the electrical activity of each stage of the cardiac electrical cycle:

- P wave: represents the atrial depolarization.
- PQ segment: is the period between the end of the P wave and the beginning of the QRS complex. It represents the delay of the electrical stimulus in the AV node and, as no myocardium is activating at that moment, the PQ segment is flat. A shortening or enlarging of this segment may indicate conduction problems in the AV node.
- QRS complex: represents the sequential activation of the ventricles. Q wave stands for the septum contraction, R wave for the lower part of the ventricles and S wave for the upper part. An enlarging of the QRS duration may indicate problems in the conduction of the Hiss bundle or its branches.
- ST segment: is the period between the end of the S wave and the beginning of the T wave. During the ST segment, all ventricular myocytes are contracted and no electrical currents occur, so this segment is flat. An elevation or depression of the ST may indicate myocardial infarction or ionic imbalance.
- T wave: represents the repolarization and the consequent relaxation of the ventricular myocardium.

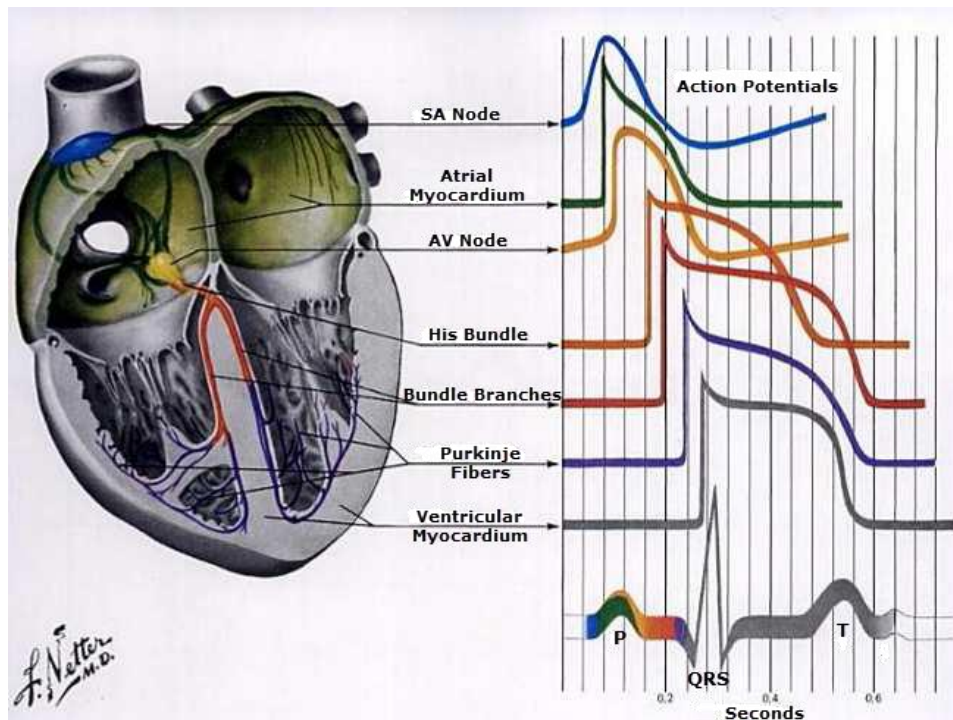


Figure 6. ECG waves [3]. Each wave of the P-QRS-T complex is related to the electrical activity of different cardiac structures. P wave: atrial depolarization. PQ segment: delay in the AV node. QRS wave: ventricular depolarization. ST segment: time during ventricular myocardium is contracted. T wave: ventricular repolarization.



Atrial Fibrillation

Atrial fibrillation (AF) is a fast arrhythmia (tachyarrhythmia) characterized by the set up of recurrent, multiple and uncoordinated electrical waves in the atrium that excite the atrial myocardium in a totally disorganized way. As a result, atrial contraction is inexistent, indeed, and instead of contracting, atrial tissue just vibrates. This has two consequences: on the one hand, the absence of atrial contraction decreases the heart beating efficiency by a 20 to 30%; on the other, the existence of erratic and recurrent activation waves in the atrium triggers arrhythmic, uncoordinated and usually fast, ventricular beats [1].

AF usually progresses from short, rare episodes, to longer and more frequent attacks. Clinically, different types of AF are distinguished, based on the presentation and duration of the arrhythmia [4]:

- **Paroxysmal AF** consists of self-terminating episodes, usually shorter than 48h.
- **Persistent AF** is present when an AF episode either lasts longer than 7 days or requires termination by cardioversion (either pharmacological or electrical).
- **Long-standing persistent AF** is considered so when it has lasted for more than 1 year.
- **Permanent AF** is said to exist when the presence of the arrhythmia is accepted both by the patient and the physician.

In general terms, a patient is usually diagnosed from paroxysmal AF and as time goes on it will evolve to sustained forms of AF. The distribution of paroxysmal AF recurrences is not random, but clustered, and AF burden (the time ratio with and without AF) can vary markedly over months or even years in individual patients. Asymptomatic AF (silent AF) is common even in symptomatic patients, irrespective of whether the initial presentation was persistent or paroxysmal.

Epidemiology and Related Pathologies

AF is the most common sustained arrhythmia, affecting 1–2% of the population. Over 6 million Europeans suffer from this arrhythmia, and its prevalence is estimated to, at least, double in the next 50 years as the population ages. AF prevalence increases with age, from 0.5% at 40–50 years, to 5–15% at 80 years. Men are more often affected



than women. The lifetime risk of developing AF is ~25% in those who have reached the age of 40 [4].

As atrial beat is inexistent during AF, blood flows passively to the ventricles, which can generate regions inside the atrium where blood hardly moves, causing the blood to coagulate, which can produce stroke and other thrombo-embolic events. In fact, AF confers 5-fold risk of stroke, and one in five of all strokes is attributed to this arrhythmia. Paroxysmal AF carries the same stroke risk as permanent or persistent AF, since AF episodes of few hours of duration are enough for thrombus formation. Ischemic strokes in association with AF are often fatal, and those patients who survive are left more disabled by their stroke and more likely to suffer a recurrence than patients with other causes of stroke. In addition to that, as a result of the irregular, fast ventricular rate, patients with AF have significantly poorer quality of life, and their exercise capacity is considerably reduced [4][5].

Symptoms and Diagnosis

Many patients with AF have no symptoms (silent AF), which makes that many of them remain undiagnosed, even an important amount of them will never present to hospital. In fact, many patients are firstly diagnosed of silent AF after suffering a cryptogenic stroke. When symptomatic, patients with AF suffer from palpitations, irregular and rapid heartbeat, fatigue (general or when exercised), faintness or confusion, dizziness or shortness of breath, among others.

An irregular pulse should always raise the suspicion of AF, but an ECG recording with at least 30 seconds duration must be done to differentiate AF from other supraventricular or ventricular arrhythmias. In an ECG recording, AF shows irregular narrow beats (supraventricular origin) and indistinguishable P wave, although some low amplitude noisy activity can be observed in the base line (especially in those leads that have good representation of atrial activity, as V₁). As an example, in panel A) of Figure 7 a normal ECG trace is shown. Panel B), shows an AF ECG recording, where irregular narrow QRS complex can be seen, while erratic low amplitude can be observed in the base line, corresponding to auricular fibrillatory activity.



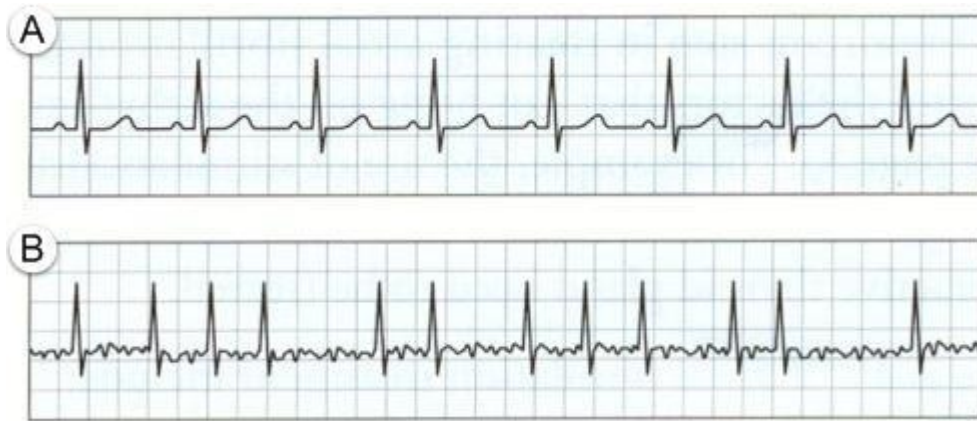


Figure 7. Normal and AF ECG. A) normal ECG trace. B) AF ECG trace, where irregular narrow QRS complexes can be seen, while erratic low amplitude can be observed in the base line, corresponding to auricular fibrillatory activity.

As mentioned above, AF episodes can self-terminate and the triggering situations of a new episode are not easily predictable. Thus, only an opportunistic ECG could find the arrhythmia. Moreover, assessment of the AF burden is important to decide the treatment or to evaluate the effectiveness of a therapy [6]. It has been estimated that 7 day Holter ECG recording or daily and symptom-activated event recordings may document the arrhythmia in approximately 70% of AF patients, and that their negative predictive value for the absence of AF is between 30 and 50% [7]. For that reason, long term (24h to 7 days) ambulatory ECG monitoring is recommended for diagnosing and controlling the evolution of patients with AF; even, in highly symptomatic patients longer monitoring times should be evaluated, including the implantation of a cardiac monitor which allows over 2 year monitoring [4][5]. Different technical alternatives for long term cardiac monitoring will be carefully discussed in the next chapter.

3. Technical Background and State of the Art

Ambulatory ECG Monitoring

Ambulatory ECG monitoring is a widely used noninvasive technique in which ECG is continuously recorded over an extended period of time, typically 24 to 48 hours, to evaluate symptoms suggestive of cardiac arrhythmias, i.e., palpitations, dizziness, or syncope. Norman J. Holter was the first one to introduce the ambulatory ECG monitoring in the 1940s, for that reason, the ECG recording of ambulatory patients is nowadays known as Holter test. The original Holter monitor was a 35 kg backpack with a reel-to-reel FM tape recorder, analog patient interface electronics and large and heavy batteries which enabled it to record a single ECG lead during several hours.[8]

Traditional Holter Test

From Norman Holter's time up to now, ambulatory ECG recorders have been gradually modified to incorporate several technological enhancements. If first Holter recorder was a 35 kg backpack with a reel-to-reel FM tape recorder, in the 1990s they had the size of a walkman and recorded the ECG on a cassette tape, and nowadays they use flashcard memory, digital electronics and their size is so reduced that they are slightly bigger than the AAA battery that they need to work. Figure 8 shows the technological evolution of Holter systems over the last decades. Holter recorders often include an event button for the patient to indicate the presence of symptoms or any other remarkable event. Once the monitor is returned, data are analyzed and correlated with marked events and symptoms.

Although technological advances have reduced size and weight of monitors, and have eased the whole process of recording and processing the signals, the medical test known as Holter has not experienced any change for a long time. It is defined as an, ideally, three lead ambulatory ECG recording, during at least 24h and no more than 48h, using adhesive and disposable electrodes wired to the recorder. [9]

One limitation of traditional Holter systems comes from the use of adhesive electrodes, which can produce allergic reactions, and wires, that may introduce noise in ECG signal when moved (and patient is expected to move in his/her daily life), so ECG



signal can be very noisy in active patients. But the main limitation is that Holter monitoring has been demonstrated to have reduced diagnostic yield [10][11], so it will be ineffective when patients experience infrequent symptoms or pathologic events. For that reason, clinical guidelines are encouraging doctors to perform longer monitoring than 24h [9], at least 7 days to achieve a good diagnostic yield for AF [7], and even more if symptoms are infrequent.

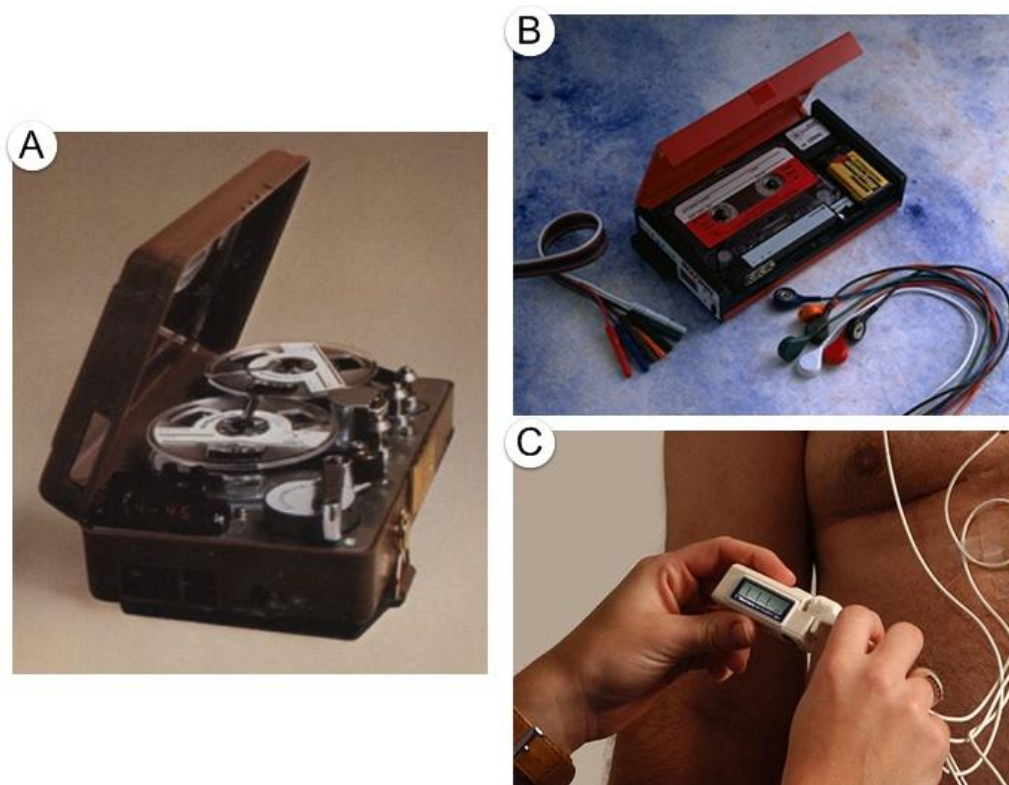


Figure 8. Evolution of Holter devices over last decades. A) Model 445 Mini-Holter Recorder, released in 1976. B) RZ151 Series Cassette Holter, released in late 1990s. C) Mortara H3+, currently on market.

Long-Term Cardiac Monitoring

Since traditional 24h Holter has limited diagnostic yield and it is proved that longer monitoring times improve the diagnostic yield [10][11], many strategies have been developed to extend monitoring times. This section will analyze each strategy and present some representative products.

Ambulatory Event Monitor

Ambulatory event monitors (AEMs) were developed to provide longer periods of monitoring than a regular Holter. They are attached to the patient by chest electrodes and they record ECG whenever activated by the patient (by pressing an event button

when any symptom is felt). Some of these devices are continuously monitoring (but not recording) the cardiac rhythm and, if a slow, fast or irregular heart rate is detected, an activation is triggered. Once activated, data are stored for a programmable fixed amount of time before the activation and a period of time after the activation.

Another less sophisticated form of event monitor is the post-event recorder. This one is not worn continuously but instead it is applied directly to the chest area once a symptom develops, so it cannot record the rhythm before the device is activated.

Both event monitors and post-event recorders usually have a looping memory. This means that the newest event will erase the oldest when memory is fully written. For this reason, these devices are also referred as event loop recorders (ELRs).

The limitations of these devices include the following. On the one hand, the patient has to be awake and coherent enough to activate the device, unless automatic event detection is build into the monitor and the automatic algorithm detects the cardiac event. On the other hand, a significant percentage of patients are noncompliant with continuous application of the devices, mostly because the skin is irritated or damaged by the electrodes and also because of poor quality signal during exercise. Finally, what maybe the most important limitation is that, in automatically triggered devices, the memory can be filled up with noisy signals as a result of false positive detections, erasing any true event recorded in the past.[8][9]

Holter Patch

Holter patch is a long-term ECG monitoring solution formed by an adhesive patch that ideally includes inside all the necessary electronics to perform a Holter-like monitoring during 7 days at least. The most mature solution in this field is ZIO® Patch, developed by iRhythm Technologies, Inc (Figure 9). The ZIO® Patch is a Food and Drug Administration-cleared compact, low-profile, noninvasive, water-resistant device that is worn for up to two weeks throughout normal activity. After using it, or after the symptoms that motivated the monitoring have appeared, the device is mailed by the patient to iRhythm for data analysis in their own data center and using a proprietary algorithm called ZIO® ECG Utilization Service (ZEUS).[12]





Figure 9. ZIO® XT Patch, by iRhythm Technologies, Inc.

iRhythm and other patch manufacturers have made a great effort in electronics miniaturization and autonomy optimization, and, of course, in developing hypoallergenic adhesives with embedded wet gel electrodes able to last up to 14 days on the skin enduring movements, sweat and water. However, it is a challenge partially achieved attending to the work of Turakhia et al. [11], where a population of 26,751 wearing ZIO® Patch was studied and the result was that 50% of the patches were only worn until day 7, and 75% until day 10 of monitoring.

Smart Fabric Holter – NUUBO

Nuubo is a Spanish SME-medical device company founded in 2005, and it focuses on cardiac monitoring solutions based on wearable medical technologies (smart fabrics), targeting the medical and sport medicine global markets.

Nuubo ECG Wearable Cardiac Monitoring System is a complete and non-invasive solution for monitoring and analysing cardiac and physical activity of an individual or group by using a biomedical garment, an electronic device and a software analysis. Nuubo's technology is based on a garment comprising a sensor with flexibility and elasticity, which allows recording good quality ECG signals, even in movement, with improved adhesion properties but avoiding adhesive elements which produce skin irritations.

BlendFix® Sensor Electrode Technology is the core sensor technology that is based on the use of flexible and elastic electrically conductive silicone materials integrated into elastomeric polymer wearable sensors “printed” into a garment for everyday use. Nuubo's core sensor technology main benefits are:

- Optimal ECG signal quality both during regular activities and sport practice.
- Easy-to-use: it does not need supervised placement, because electrodes are placed on an easy to vest wearable.

- **Comfortable:** elasticity drives both comfort and adaptability to the normal thoracic chamber movements, enabling the patients to comfortably perform real day-to-day activities and sports specially.
- **Sensing versatility:** electrodes can be printed onto almost any textile, and in any form or size.
- **Very low manufacturing cost.**

Nuubo has received CE-Mark approval for the commercial sale of both single-lead and multi-lead solution. These product solutions are compliant with Medical Device Directive 93/42/EEC, and the company is also certified as a medical device company by ISO 9001 and ISO 13485.

Nuubo's portfolio offers different solutions to cover the ECG monitoring from 7 to 60 days, both for regular and sportive activity, using 1 or 3 leads. Nuubo's products have been proved to achieve high patient's compliance with ECG signal of excellent quality [13][14] and to be of great utility in sport medicine [15][16]. In Figure 10 a sample of Nuubo's portfolio is shown.

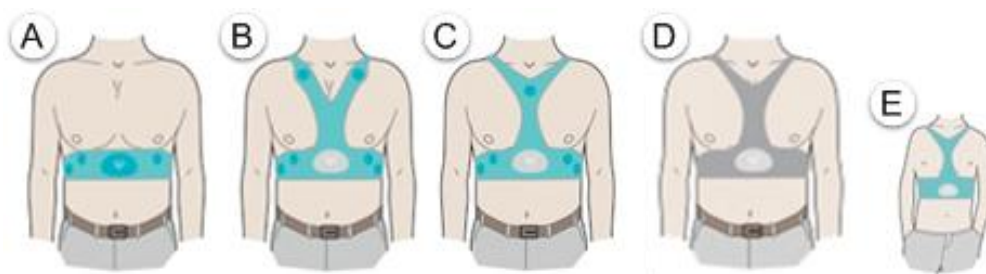


Figure 10. Sample of Nuubo's portfolio. A) 1 lead wearable, designed for longer than 4 weeks monitoring. B and C) Two concepts of 3 lead wearable, for 1 or 4 weeks respectively. D) 3 lead wearable specially designed for sportive activity. E) 3 lead wearable conceived for pediatrics monitoring.

Mobile Cardiac Telemetry

Mobile Cardiac Telemetry (MCT) refers to a concept that comprises all the systems involved in a real-time continuous attended cardiac monitoring service. MCT is designed to combine the benefits and avoid the limitations of Holter monitors and standard ELRs.

They are worn continuously and are similar in size to the standard ELR. They continuously record the ECG signal of ambulatory patients and automatically generate and transmit an arrhythmic event. Those events can be patient or event-activated. Events are transmitted usually to a secondary device which communicates by cellular



phone network with a monitoring station, where trained staff members analyze live incoming patient's data and inform the referring physician according to previously defined criteria.[8]

For example, CardioNet Inc. is a company that offers mobile cardiac outpatient telemetry. In this system, called Mobile Cardiac Outpatient Telemetry™ (MCOT™), the patient wears a 3-lead sensor, which constantly communicates with the MCOT monitor, a lightweight unit that can be carried in a pocket or a purse. When an arrhythmia is detected according to preset parameters, the ECG is automatically transmitted to a central CardioNet service center, where the ECG is immediately interpreted and results sent to the referring physician. The referring physician can request the level and timing of response, ranging from daily reports to immediate results.

A similar approach has been developed by Medtronic with the product called SEEQ, which instead of using wired adhesive electrodes, incorporates the recording electronics in an adhesive patch that communicates with a secondary device responsible of sending events to the monitoring station. In Figure 11, MCOT of CardioNet and SEEQ of Medtronic are shown. Both products can monitor up to 30 days, but MCOT must be recharged during the process and SEEQ patches must be replaced, since one single patch has only 7.5 days of autonomy, while its secondary device has 8 hours of autonomy and should be recharged.



Figure 11. Mobile cardiac telemetry devices. Secondary communication devices can be noticed. Left: MCOT (CardioNet Inc.). Right: SEEQ (Medtronic), on the top right corner a detail of the electrodes embedded in the patch is shown.

Very Long-Term Cardiac Monitoring: Implantable Loop Recorder

Implantable Loop Recorders (ILRs) are implanted beneath the skin through a small incision of about 2 cm in the left precordial region. They are equipped with a looping memory and they are either automatically-triggered or patient-triggered by using an external activator at the moment the symptoms arise. Once activated, they record one-lead electrocardiographic trace for several minutes before and after the event.

In general, monitoring lasts either until a diagnosis is reached or until the battery runs down, which can last up to 36 months. When completion of monitoring is achieved, the device is removed from the patient. The newest generation of these devices allows remote transmission of data to a communication base which transmits data to a monitoring center by using wired or cellular phone networks. Besides, many pacemakers and implantable cardio-defibrillators incorporate this monitoring functionality. [9]

One of the most important devices of this category is Reveal LINQ, manufactured by Medtronic, which is the smallest ILR in the market. Its dimensions are 45 mm x 7 mm x 4 mm (see Figure 12), its weight is lower than 3 grams and its autonomy can reach up to 3 years. It is able to record up to 30 minutes of patient-activated events and 27 minutes of automatically-triggered events.

Complications related to the surgical procedure were one of the main limitations of these devices, but these have been highly mitigated by simplifying the procedure, that is now reduced to a simple insertion (Figure 12). This fact decreases implanting times and clinical resources involved in the procedure, which means saving economical resources to health systems. However, the most important limitation of these devices is still price, considering that the reimbursement of Medicare Services comes to near \$7,000 for the whole procedure [17].



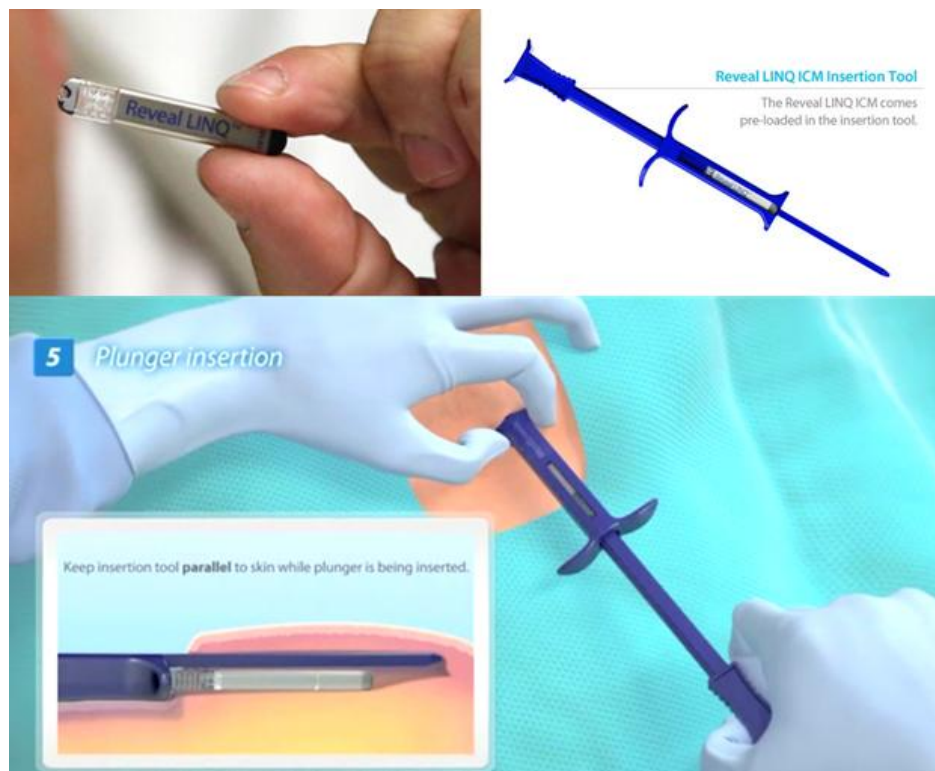


Figure 12. Reveal LINQ of Medtronic. Upper left, Reveal Linq is shown to appreciate its reduced size. Upper right, insertion tool is shown. Bottom, insertion procedure is shown.

In this section, several cardiac monitoring solutions focused on different monitoring times have been presented. In Figure 13 the monitoring time of each discussed product is shown. All these products have in common the need of ECG algorithms to assess the presence of an assortment of pathologies, either ECG is processed in real-time, as ELRs, or offline, as Holters. One of these pathologies is AF. In the next section several detection strategies will be discussed and different approaches to the problem, both from academy and industry points of view, will be analyzed.

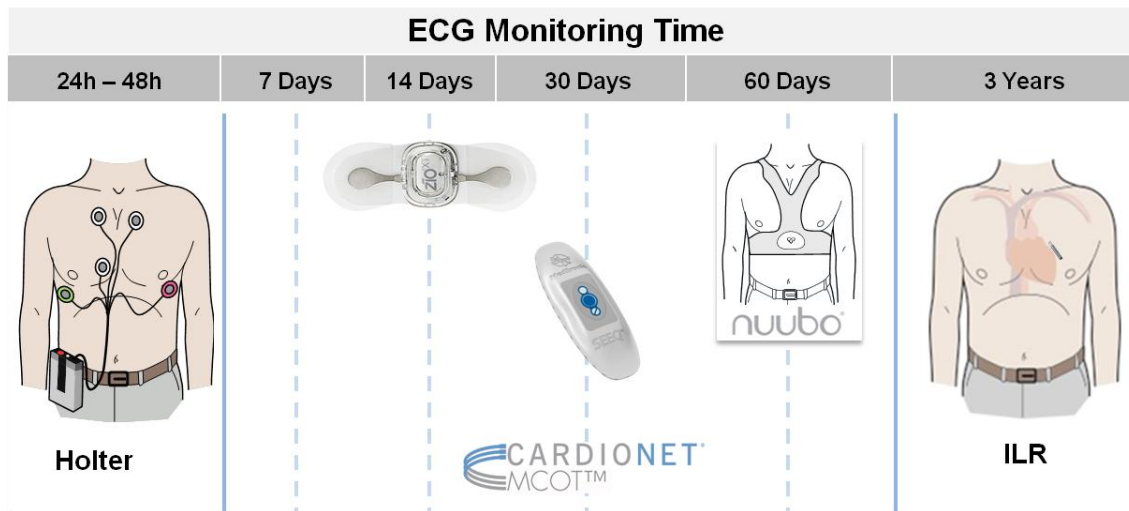


Figure 13. ECG Monitoring Time of different products, from 24h-48h of traditional Holter, to 3 years of implantable loop recorders (ILRs).

Atrial Fibrillation Detection

As it was discussed previously AF shows irregular narrow beats (supraventricular origin) and indistinguishable P wave on an ECG recording. However, some low amplitude activity can be observed on the base line, depending on the electrocardiographic lead. So, in order to detect AF on an ECG it seems obvious that been able to detect beats on the ECG is a necessity. Several QRS detectors have been developed achieving very good detection rates [18][19].

Once QRS is detected, position of R wave, which is usually the highest positive wave of the QRS, must be determined. Then, the interbeat interval, known as RR interval, is calculated. Automatic AF detection algorithms employ RR intervals to assess their irregularity in order to determine whether AF is present or not. Occasionally, some detectors also perform atrial activity analysis to make a more robust detection, but this feature is highly lead-dependent and very susceptible to noise.

In next sections, the evaluation methods and databases used to asses AF detectors will be discussed. Then, some published detectors will be reviewed and the results of some commercial products which incorporate AF detection will be shown.



Evaluation of AF detectors

The evaluation of AF detectors is a controversial topic. Several results have been published using private databases, which make results impossible to reproduce. In addition to that, different evaluation methods are used to assess the performance of the detectors, as per patient detection or elimination from the statistics of those episodes shorter than the evaluation interval used by the detector. Consider [20], [21] and [22] as a brief sample.

When public databases are used, MIT-BIH Arrhythmia Database and MIT-BIH Atrial Fibrillation Database are commonly employed. Both are described below.

MIT-BIH Arrhythmia Database

MIT-BIH Arrhythmia Database (MITDB from this point on) is a widely used public database which is freely available from PhysioNet [23], and comprises 48 fully annotated records. Annotations were done by two independent cardiologists, and when any discrepancy was found, it was solved by consensus. Annotations comprise beat annotations with its position and type label, and also rhythm labels, signal quality labels, and comments.

The source of the ECGs included in the MITDB is a set of over 4000 long-term Holter recordings that were obtained by the Beth Israel Hospital Arrhythmia Laboratory between 1975 and 1979. The database contains 23 records (numbered from 100 to 124 inclusive with some numbers missing) chosen at random from this set, and 25 records (numbered from 200 to 234 inclusive, again with some numbers missing) selected from the same set to include a variety of rare but clinically important phenomena that would not be well-represented by a small random sample of Holter recordings. Each of the 48 records is slightly over 30 minutes long.

The first group is intended to serve as a representative sample of the variety of waveforms and artifact that an arrhythmia detector might encounter in routine clinical use. The records in the second group were chosen to include complex ventricular, junctional, and supraventricular arrhythmias and conduction abnormalities. Several of these records were selected because features of the rhythm, QRS morphology variation, or signal quality may be expected to present significant difficulty to arrhythmia detectors. [24]

Attending to AF, only 7 records of MITDB contain paroxysmal AF, and all episodes totalized count 1 hour and 43 minutes. Besides, different kinds of complex



pathologic rhythms are included in MITDB, which joined to the low prevalence, make it a difficult database to test AF.

MIT-BIH Atrial Fibrillation Database

Firstly developed for [25], MIT-BIH Atrial Fibrillation Database (AFDB from this point on) is formed by 23 records of 10 hours of duration, selected from a library of over 8000 24 hours Holter recordings collected by the Arrhythmia Laboratory of Beth Israel Hospital. A total of 93 hours of AF is contained in AFDB, mostly paroxysmal episodes.

Only AF, atrial flutter, junctional flutter and normal rhythm (used to indicate all other rhythms) are labeled. Besides, two beat annotation files were prepared. First file was prepared using an automated QRS detector without correcting the results, which may be useful for studies of methods of automated AF detection where such methods must be robust with respect to typical QRS detection errors. Second file includes manually corrected beat annotations, which may be preferred for basic studies of AF itself, where QRS detection errors would be confounding. Both beat annotation files only contain the position of the R peak of the QRS, but beats are not classified by types.

Academic Solutions

In this section a review through several published AF detectors is shown. Only those algorithms showing results on MITDB or AFDB have been selected. Table 1 shows a comparative study of the results. Brief description of each algorithm is provided below.

Moody et al [25] employ a hidden Markov model (HMM) to represent an RR interval sequence using three states: short, normal or long with respect to a sliding average. The HMM was trained using a subset of MITDB selected to contain AF, normal sinus rhythm and other rhythms considered likely to confuse an AF detector. It was tested on AFDB, originally created for this publication.

Artis et al [26] use the three-state modeling employed by Moody in [25] to feed an artificial neural network (ANN) to classify a segment of RR intervals into AF or no AF categories. After that, a sliding averaging postprocessing is performed to detect transitions. It was trained and tested using the same databases as Moody in [25].

Young et al. [27] use a HMM with 2 states (AF or no AF) with a sequence of 3 RR intervals classified in 7 categories, in a similar way as Moody did in [25]. HMM



output is a low pass filtered to make delineation of AF episodes easier. The algorithm was trained and tested using the same databases as Moody did in [25].

Tatento and Glass, in 2000 [28], proposed an algorithm that used the Kolmogorov-Smirnov (KS) test to assess the irregularity of ΔRR (difference between consecutive RR intervals) calculated on a sequence of 100 consecutive beats. AFDB was used to train the algorithm and a subset of MITDB (containing only the signals with AF) was used for test. One year after, they published a more detailed and depurated version of the algorithm [29], that was tested on full MITDB and obtained better results than in the first one.

Ghodrati and Marinello [30] proposed in 2008 a method based on modeling the RR interval as both Gaussian and Laplace probability density function, and then applying Neyman-Pearson detection criteria. MITDB was used for training and AFDB for testing.

Couceiro et al. [31] used an artificial neural network classifier which received three inputs: RR irregularity assessment based in HMM in a similar way to Moody's in [25], ratio of detected P waves and spectral analysis of the atrial activity after performing QRS-T cancellation. A subset of AFDB was used to train the algorithm and complete AFDB was used for testing.

Sarkar et al. [32] proposed a computationally simple AF detector based on statistical analysis of the histogram of the Lorentz plot of ΔRR . They used an AFDB subset and a private database to search the thresholds that optimized the area under curve (AUC) ROC (Receiver Operating Curve). It was tested on full AFDB, MIT-BIH Normal Sinus Rhythm Database (NSRDB), Normal Sinus Rhythm RR Interval Database (NSRDB_RR) from Physionet and other private databases.

In 2009, Dash et al. [33] developed a detector based on a statistical approach. Their detector calculates turning points ratio, root mean square of successive differences and Shannon entropy of 128 consecutive RR intervals. Thresholds were found by maximizing AUC. They used AFDB and MITDB both for testing and training the algorithm.

In the same year, Babaeizadeh et al. [34] published a detector that uses HMM to produce an AF score that is enhanced by adding atrial activity analysis. They used private database to develop the algorithm and they tested it on AFDB.

Huang et al. [35] proposed an algorithm to detect transitions between AF and sinus rhythm by using a statistical analysis based on KS test of the preprocessed ΔRR sequence. AFDB and other private database were used to train, and NSRDB and private database to test.

Lian et al. [36] developed method is based on counting non null bins of the histogram of RR vs. ΔRR . They used AFDB, NSRDB, NSRDB_RR and MIT-BIH Long Term Atrial Fibrillation Database (LTAfDB) to find the threshold that maximizes AUC, and tested on the same databases.

Zhou et al. [37] published last year an interesting approach that assesses the irregularity of RR by using the entropy of symbolic dynamics of the sequence. For this, after preprocessing, ΔRR is transformed to ten different symbols and 3-symbol words are then analyzed to detect transitions between AF and other rhythms. LTAfDB was used to train and AFDB, MITDB and NSRDB were used to test.

And finally, this year, Petrénas et al. [38] presented a low-complexity detector based on statistical analysis of RR sequence. An ectopic correction method is incorporated and short windows of 8 beats are used to detect transitions. LTAfDB was used to train and AFDB, and NSRDB were used to test.

Results and other details of each algorithm can be found in Table 1. Observe that results in *italics* have been obtained using training database and **bold** results have been obtained using test database.



Table 1. Comparative of several published AF detectors. Italics indicates results on training database, bold indicates results on test database.

Author	Year	Features	Technique	Comments	Analyzed Segment	MITDB			AFDB		
						Sens	Spec	+P	Sens	Spec	+P
Moody [25]	1983	Characterizes each RR as short, normal or long regarding a sliding average.	HMM	Train: MITDB subset. Test: AFDB.	20 beats	<i>96.09</i>	--	<i>86.79</i>	90.65	--	82.38
Artis [26]	1992	Same as Moody	ANN	Train: MITDB subset. Test: AFDB.	An sliding window postprocessing is applied to detect transitions.	--	--	--	92.86	--	92.34
Young [27]	1999	Same as Moody, but using 7 categories. Ventricular ectopics are excluded.	HMM	Train: MITDB subset. Test: AFDB.	4 beats (detects transitions)	<i>97.7</i>	<i>88.73</i>	<i>86.77</i>	94.75	93.51	91.38
Tatento [28]	2000	Δ RR histogram	Statistical analysis	Train: AFDB. Test: MITDB subset	100 consecutive beats	88.80	64.10	--	<i>93.20</i>	<i>96.70</i>	<i>95.20</i>
Tatento [29]	2001	Δ RR histogram	Statistical analysis	Train: AFDB. Test: MITDB.	100 consecutive beats	88.17	93.56	62.33	<i>94.40</i>	<i>97.20</i>	<i>96.10</i>
Ghodrati [30]	2008	Δ RR normalized. Only normal beats were considered.	Statistical analysis. Threshold to optimize AUC.	Train: MITDB. Test: AFDB.	30 beats	<i>92.00</i>	--	<i>73.00</i>	89.00	--	87.00
Couceiro [31]	2008	HMM as Moody +Spectral Analysis of atrial activity (QRST cancel) +P wave detection	ANN	Train: AFDB subset. Test: full AFDB, NSRDB and NSRDB_RR	12 beats	--	--	--	93.80	96.09	--
Sarkar [32]	2008	Histogram of Δ RR Lorentz plot.	Statistical analysis	Train: AFDB subset + private database. Test: complete AFDB + private database.	2 minutes	--	--	--	97.50	99.00	95.80

Author	Year	Features	Technique	Comments	Analyzed Segment	MITDB			AFDB		
						Sens	Spec	+P	Sens	Spec	+P
Dash [33]	2009	RR. Ectopics correction	Statistical analysis. Threshold to optimize AUC.	Test: AFDB and MITDB Train: AFDB and MITDB	128 consecutive beats	90.20	91.20	--	94.40	95.10	--
Babaeizadeh [34]	2009	RR and P-wave.	HMM process RR, and its output is combined with P-wave analysis.	Train: private database. Shorter episodes than 1min are ignored for evaluation proposes.	Detects transitions	--	--	--	94.00	99.00	98.00
Huang [35]	2011	Preprocessed Δ RR	Statistical analysis. Threshold to optimize AUC.	Train: AFDB and private database. Test: NSRDB and private databases.	Detects transitions	--	--	--	<i>96.10</i>	<i>98.10</i>	--
Lian [36]	2011	Histogram RR vs Δ RR	Statistical analysis. Threshold to optimize AUC.	Train: MITDB, AFDB, NSRDB and NSRDB_RR. Test on same train databases.	128 consecutive beats	98.90	78.80	--	95.80	96.40	--
Zhou [37]	2014	Preprocessed RR and Δ RR	Entropy of symbolic analysis.	Train: LTAFDB Test: AFDB, MITDB and NSRDB	Detects transitions	97.33	90.78	55.29	96.89	98.25	97.62
Petrénas [38]	2015	Preprocessed RR. Ectopic correction	Statistical analysis. Threshold to optimize AUC.	Train: LTAFDB. Test: AFDB and NSRDB	Detects transitions with 8 beat windows	--	--	--	97.00	98.30	--

Abbreviations HMM: Hidden Markov Model; ANN: Artificial Neural Networks; AUC: Area Under the Curve ROC; LTAFDB: MIT-BIH Long Term Atrial Fibrillation Database; NSRDB: MIT-BIH Normal Sinus Rhythm Database; NSRDB_RR: Normal Sinus Rhythm RR Interval Database;



To sum up, several AF detection algorithms have been discussed. They use different approaches to analyze RR irregularity, as HMM, ANN, statistical analysis or symbolic dynamics analysis. Some of them perform ectopic correction to remove irregularity sources that can be confused with AF irregularity. Also, some other methods use atrial activity assessment to add more information to the RR irregularity evaluation in order to make more informed decisions. However, results are not better than those obtained without using it.

First detectors, especially those detectors inspired in Moody's [25] methodology, commonly employ MITDB to train the algorithms and AFDB to test. Detectors using MITDB as test database have quite low positive predictivity, while those using AFDB as test database have higher statistics, clearly showing that MITDB is a more difficult database for an AF detector than AFDB one, as discussed in previous sections. In addition to that, using the same databases for training and testing is a recurrent methodological mistake.

Industrial Solutions

Regulations and Standards

In general, commercial products must comply with several standards to ensure that their essential workings fulfill some specific features that make the product safe for the expected use. This fact becomes especially important when it comes to medical products. In particular, in the case of ambulatory electrocardiographs the standard that applies is *IEC 60601-2-47:2012 – Medical electrical equipment – Part 2-47: Particular requirements for the basic safety and essential performance of ambulatory electrocardiographic systems*. Among many other features, the evaluation method for AF detection is well defined in this standard.

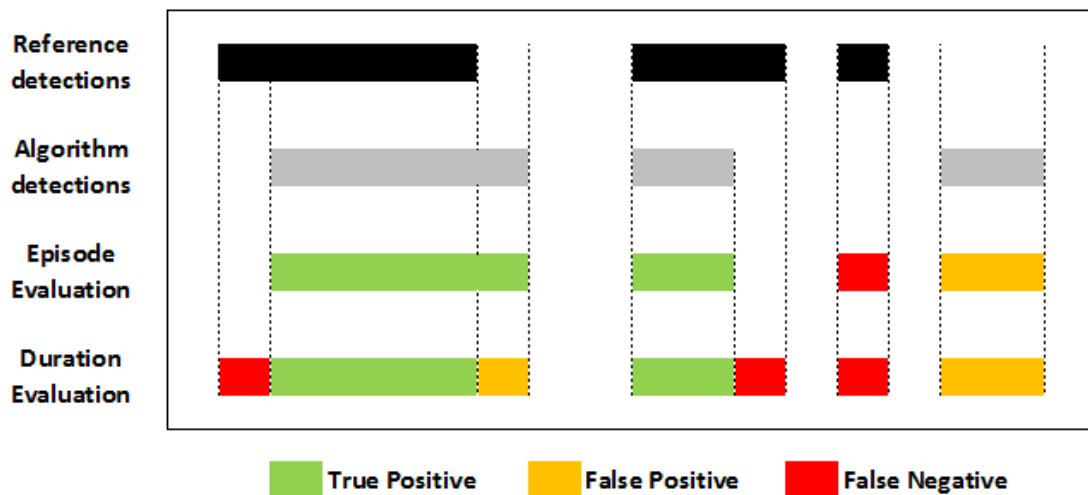


Figure 14. Graphical representation of the evaluation method attending both to episode and duration evaluation as defined in IEC 60601-2-47:2012.

The standard specifies that sensitivity and positive predictivity must be calculated both for AF episode and its duration:

Measurement of AF episode sensitivity and positive predictivity: each reference episode for which overlap exists is counted as a true positive for purposes of determining AF episode sensitivity; any other reference episodes are counted as false negatives. Similarly, each algorithm-marked episode for which overlap exists is counted as a true positive for purposes of determining AF episode positive predictivity; any other algorithm-marked episodes are counted as false positives.

Measurement of AF duration sensitivity and positive predictivity requires determination of the total duration of reference and algorithm-marked VF and of the total duration of periods of overlap as defined above.[39]

Figure 14 shows a graphical representation of the evaluation method attending both to the episode and the duration statistics defined above.

The standard also specifies that MIT-BIH Arrhythmia Database must be used for evaluating AF detection, although it is not specified if this database must be used during to train the system or not.

Commercial Products

Despite AF evaluation is clearly disclosed in the standard, AF detection statistics of a commercial product are susceptible data and so they are not clearly disclosed. For example, AliveCor is a company that have developed an FDA-cleared mobile phone case with built-in electrodes to record short ECGs from the fingers of the patient. Their product is aimed to be a tool for detection and control of AF patients, in order to reduce the associated morbidity and mortality. However, no AF detection statistics are disclosed in their corporative web page.

In this section, AF detection results of some commercial products are disclosed. Table 2 shows a comparative of AF detection results of several commercial products which results have been published. GE Marquett 12SL is a diagnosis algorithm for 12-lead ECG developed by General Electric. Kinetic™ AF ECG Algorithm is part of a family of algorithms to process ECG developed by Monebo Technologies, who licenses its algorithms to third parties, as CardioComm Solutions Inc. or Freescale Semiconductors. DLX ECG Algorithm is used by Philips in different cardiac monitoring solutions. Reveal LINQ and SEEQ are both products from Medtronic and have been reviewed previously.

Table 2. Comparative of AF detection results of several commercial products.

	Sens (%)	+P (%)	Database
GE Marquett 12SL	87.5	95.4	Private: 10761 records.
Kinetic™ AF ECG Algorithm	95.7	83.3	Private: 250 records.
DLX ECG Algorithm	89.0	90.0	Private: 1785 records.
Reveal LINQ	97.4	84.4	Private: 150 records.
SEEQ (Medtronic)	90.0	85.0	MITDB, as specified in <i>IEC 60601-2-47</i> (duration assesment)

As it can be seen, all products except SEEQ use private database, so compare results is not possible. To our concern, only SEEQ shows AF detection results on MITDB but it is not disclosed if this database was only used for testing or was also used for training the algorithm. However, it seems obvious that Medtronic, after doing their best for the development of their AF detector, would had performed a last train of the system including MITDB in the training data to obtain the best possible performance.

Moreover, they also declare that the statistics stands for the duration assessment and the evaluation has been performed as specified in standard *IEC 60601-2-47*.

Performance Goals

As it was declared, the main objective of this Master Thesis is to develop a classification system able to distinguish between AF and non-AF rhythms.

AF is clinically defined as an irregular cardiac rhythm of narrow beats (supraventricular origin) where no P wave can be distinguished maintained during 30 seconds at least [4]. Therefore, the developed system should only use the inter-beat intervals information contained in 30 seconds segments of ECG signal to perform the classification. Thus, no morphology assessed rejection should be made to eliminate ectopic beats that can be confused with AF rhythm and every beat should be considered to generate the RR interval. This way, the classifier could be integrated in any ECG analysis system that performs beat detection, such as implantable or external cardiac monitors or offline analysis platforms as holter analysis software.

The performance goal of this development is to overcome the results of SEEQ, which is, to our concern, the only commercial product shown AF detection statistics based on *IEC 60601-2-47* standard and public database. In other words, the objective is to reach sensitivity higher than 90% and positive predictivity higher than 85% on MITDB.

To achieve this goal, artificial neural networks will be used and several strategies to improve the learning and generalization will be explored.





4. Methods

Artificial Neural Networks

Artificial Neural Networks (ANNs) are a family of statistical learning models inspired by biological neural networks, which are formed by millions of interconnected neurons. Natural neurons receive signals through synapses located on the dendrites or the soma of the neuron, and, whenever the signal received is strong enough, the neuron is activated and a signal is emitted through the axon. This signal might be sent to another synapse and might activate other neurons of the network.

An ANN is composed of basic nodes, units or artificial neurons connected together forming a network. An artificial neuron is a computational model, that mimics the functioning of biological neurons: several inputs are received, the artificial neuron performs a weighted sum of them and the result is usually passed through a non-linear function (known as activation function) to produce the output. A scheme of an artificial neuron can be seen in Figure 15.

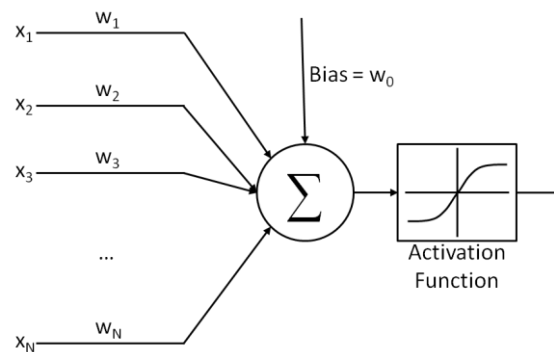


Figure 15. Scheme of an artificial neuron.

Firstly presented by Rosenblat in the 1950s [40], a perceptron is a neuron that uses the step function as activation function. Thus, for an input $X = \{x_1, \dots, x_I\}$ and a set of weights $W = \{w_0, \dots, w_I\}$, perceptron output u is defined as follows:

$$y(X) = w_0 + \sum_{i=1}^I w_i x_i$$
$$u(y) = \text{step}(y) = \begin{cases} 1, & \text{if } y > 0 \\ 0, & \text{if } y \leq 0 \end{cases} \quad (1)$$



It has been proved that a perceptron can correctly classify samples of two classes if they are lineally separable; in other words, a perceptron is able to determine hyperplane-shaped borders to distinguish between two classes [41]. To learn the weights of a perceptron from classified samples, a gradient descent optimization can be used, but the step function discontinuity and the null derivative generate numerical problems. So continuously differentiable sigmoid-shaped functions, such as logistic function or hyperbolic tangent, are generally used instead of the step function.

Since McCulloch and Pitts proposed the first neural network model [42], many other different models have been developed under the same philosophy. The most typical configuration is the feed-forward, layered network called multilayer perceptron (MLP), where neurons are arranged in layers, and a layer input is only connected with the immediately previous layer output. A MLP consists of three or more layers, the input and output layers and the hidden layers, which are not accessible from the outside of the network. An example of a three layer MLP is shown in Figure 16.

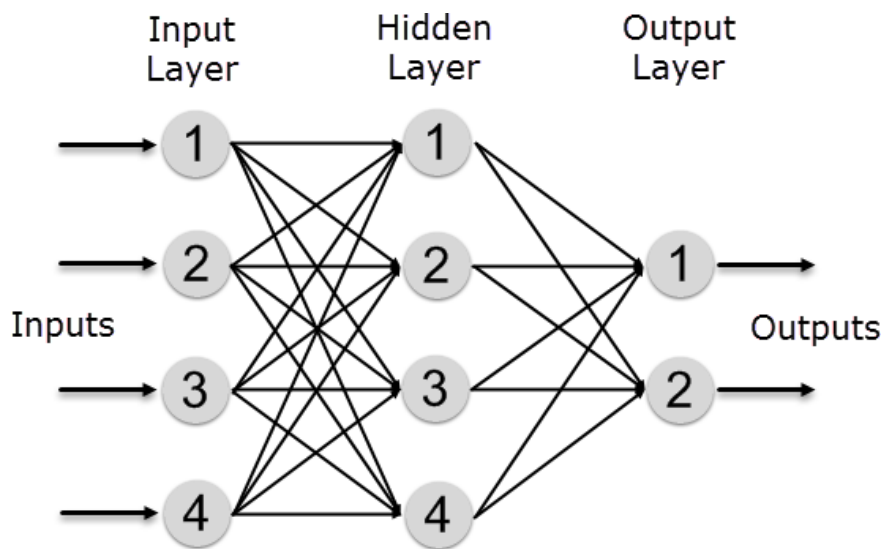


Figure 16. Multilayer perceptron with one hidden layer diagram, where each circle represent one unit or neuron.

It has been proved that any arbitrary decision region can be arbitrarily well approximated by feed-forward neural networks with only a single hidden layer with enough number of neurons using any continuous sigmoidal nonlinear activation function [43].

Backpropagation

A key step in using an MLP model is to choose the optimal weights that represent the problem. Backpropagation method, proposed by Rumelhart et al in 1986 [44], is commonly used for that task. The basic idea of this method is to backpropagate the errors in order to modify each weight by applying gradient descent to them. In order to calculate the error, backpropagation requires a known desired output for each input sample, so labeled samples are needed for training.

Let say that the neural network computes a function $M(Z^p, W)$, where Z^p refers to the p -th input sample, and W represents the collection of adjustable parameters in the system. An error function $E^p = C(D^p, M(Z^p, W))$, measures de discrepancy between the desired output D^p for the sample Z^p and the output produced by the system. The sum of the squared differences is usually employed as an error measure, but any other function can be used. Thus, each weight w_{ij}^n (weight i of the neuron j of the layer n) should be modified as follows:

$$w_{ij}^n(t+1) = w_{ij}^n(t) - \Delta w_{ij}^n(t+1) = w_{ij}^n(t) - \eta \frac{\partial E(t+1)}{\partial w_{ij}^n} \quad (2)$$

Where η is the learning rate, and E can be the error of one sample (E^p), the average error of a subset of the training dataset or the average error of the whole training dataset. Weights can be updated using these different errors, leading to stochastic, mini-batch or batch learning, respectively.

Once error is computed, Δw_{ij}^n can be calculated by using the chain rule for partial derivation. For example, if a simplified case of one output neuron is considered, error E^p only depends on scalars d^p , the desired output, and $m(Z^p, W)$, the output of the system. $mm(Z^p, W)$ can be written as a function of the last neuron inputs using equation (1).

$$E^p = C(d^p, m(Z^p, W)) = C(d^p, u(y(W_N, X_{N-1}))) \quad (3)$$

Where X_{N-1} refers to the output of the previous layer, which is the input of layer N as well. Thus, the partial derivative of the error with respect to w_{ij}^N is:

$$\frac{\partial E}{\partial w_i^N} = \frac{\partial C(d^p, u(y(X_{N-1})))}{\partial w_i^N} = \frac{\partial C(d^p, u(y))}{\partial u} \cdot \frac{\partial u(y)}{\partial y} \cdot \frac{\partial y(W_N, X_{N-1})}{\partial w_i^N} = \quad (4)$$



$$\begin{aligned}
 &= \frac{\partial C(d^p, u(y))}{\partial u} \cdot \frac{\partial u(y)}{\partial y} \cdot \frac{\partial (w_0 + \sum_{i=1}^N w_i x_i)}{\partial w_i^N} = \\
 &= \begin{cases} \frac{\partial C(d^p, u(y))}{\partial u} \cdot \frac{\partial u(y)}{\partial y} & , \text{if } i = 0 \\ \frac{\partial C(d^p, u(y))}{\partial u} \cdot \frac{\partial u(y)}{\partial y} \cdot x_i & , \text{if } i > 0 \end{cases}
 \end{aligned}$$

This procedure can be continued to determine the update term of any other weight of any other layer just by backpropagating the partial derivative of the error.

The election of the activation function is of great importance to optimize the learning process. For example, using logistic or hyperbolic tangent is very efficient because their derivatives are defined in terms of the non differentiated function, and this value was calculated while evaluating the sample, so no computation is needed to calculate the derivative of the activation function:

$$\text{Logistic function: } f_L(x) = \frac{1}{1+\exp(-x)} \quad f'_L(x) = f_L(x)(1 - f_L(x)) \quad (5)$$

$$\text{Hyperbolic Tangent: } \tanh(x) = \frac{\exp(x)-\exp(-x)}{\exp(x)+\exp(-x)} \quad \tanh'(x) = 1 - (\tanh(x))^2 \quad (6)$$

Output Units for Classification

When an ANN is used as a classifier, output neurons generally implement *softmax* activation function instead of sigmoid. The main advantage of using *softmax* is that it produces an output that can be interpreted as posteriori probability of belonging to a particular class.

Softmax function is a transformation that normalizes a K-dimensional vector \mathbf{z} of arbitrary real values to a K-dimensional vector $f_S(\mathbf{Z})$ of real values in the range [0, 1]. It is defined as follows:

$$f_S(z_j) = \frac{e^{z_j}}{\sum_{k=1}^K e^{z_k}} \quad (7)$$

If squared difference is taken as an error function, it is easy to see that gradient of the error is complicated and propagated errors will depend on the activations of all neighbor neurons, which is quite inconvenient for the computational performance of the learning process. However, if cross-entropy is used as an error function, it can be demonstrated that the gradient of the error turns into a linear function of the desired



values and the output of the network. This is the reason why, whenever *softmax* function is used as activation function of the output neurons, cross-entropy is employed as error function. Besides, optimizing cross-entropy usually produces better classification errors because it tends to allow errors to change weights even when nodes are saturated [45].

Approaches to Improve Learning

In this section, several strategies to improve learning capabilities of an ANN are disclosed. Those strategies enhance learning by using momentum or tuning the learning rate of each layer, exploring the use of activation functions different from usual sigmoids, and also regularizing the value of weights, as well as more complicated strategies as dropout.

Momentum

When the error surface is highly nonspherical, learning can be very slow because the learning rate must be kept small to prevent divergence. The use of momentum can increase convergence speed because it damps the size of the steps along directions of high curvature. This yields a larger effective learning rate along the directions of low curvature [46]. Momentum adds a fraction of previous weight update to the current one, modifying the learning equation defined in equation (2):

$$w_{ij}^n(t+1) = w_{ij}^n(t) - \eta \frac{\partial E(t+1)}{\partial w_{ij}^n} - \mu \Delta w_{ij}^n(t) \quad (8)$$

μ denotes the strength of the momentum term.

Learning Rate Scaling

In most neural net architectures, the second derivative [46] of the error function with respect to weights in the lower layers is generally smaller than that of the higher layers (considering higher layers the ones nearer to the output –see Figure 17–). As it is shown in equation (4), the update term of a weight of the highest layer contains the derivative of the activation function, which is between zero and one for usual sigmoids as seen in equations (5) and (6). The update term of weights of lower layers will be multiplied by more sigmoid derivatives, making the backpropagated error smaller when lower weights are updated. For this reason, weights in the lower layers will converge to their optimal value in a slower way than weights in the upper layers.



Because of this, LeCun et al. [46] recommend that learning rates in the lower layers should generally be larger than in the higher ones. In this Master Thesis, a coefficient of 2 has been used, so the learning rate of one layer is twice as large as the immediate higher one.

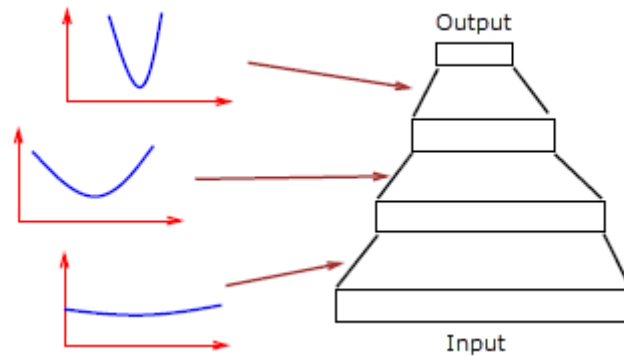


Figure 17. In a multilayered architecture, generally the second derivative of the error function is often smaller in lower layers [46].

Rectified Linear Unit

Non-linear, bounded activation functions as hyperbolic tangent or logistic function have been traditionally used in neural networks. However, in last years it has been demonstrated that using different activation functions can lead to better results. In particular, the use of Rectified Linear Units (ReLU) has been proved of great interest [47][48]. ReLUs are neurons that activate using rectified linear function, which is defined as follows:

$$f_{ReLU}(x) = \max(x, 0)$$

$$f'_{ReLU}(x) = \begin{cases} 1 & \text{if } x > 0 \\ 0 & \text{if } x \leq 0 \end{cases} \quad (9)$$

Differences between logistic function and ReLU can be appreciated in Figure 18.

The use of ReLUs has several advantages. First, the convergence is faster than using regular logistic neural net with the same topology because the derivative is one when the function is not null. Second, ReLUs are faster to compute because no exponentiation and division is required. Zeiler et al [47] experienced an overall speed up of 25% in their tests. Third, networks using ReLUs generalize better than its logistic counterpart. This is because the internal representation produced by the network is much more regularized. Unlike logistic units that produce small positive values when the input is not aligned with the internal weights, rectified linear units often output

exact zeros. Improved generalization can be seen as the effect of the increased sparsity of the internal representation.

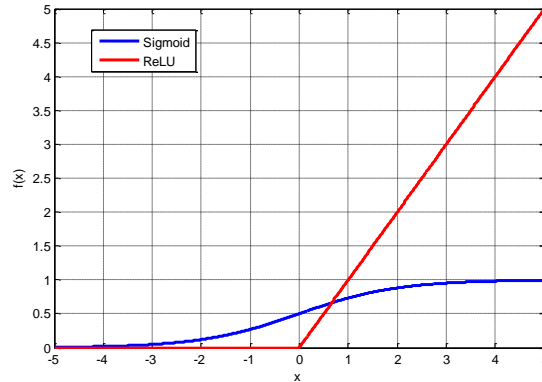


Figure 18. Logistic (blue) and ReLU (red) graph.

Max-norm regularization

However, using ReLU can lead to weights of huge value, creating difficulties for convergence; this is why it is interesting to regularize the value of weights vectors of each neuron. Max-norm regularization has been found to be especially useful in combination with ReLU and also with dropout [48], which will be described in the next section. Max-norm regularization is based on using an upper bound for the norm of the weight vector of each hidden unit. In particular, if W_j^n is the vector of weights incident to j neuron of n layer, network training is performed under the constraint $\|W_j^n\|_2 \leq c$, where c is the maximum norm permitted for any vector of weights. During training, whenever any weight norm is higher than c , the vector is renormalized to norm c by using this transformation:

$$W_j^n = \begin{cases} \frac{W_j^n \cdot c}{\|W_j^n\|_2} & \text{if } \|W_j^n\|_2 > c \\ W_j^n & \text{if } \|W_j^n\|_2 \leq c \end{cases} \quad (10)$$

The use of max-norm regularization usually improves performance of neural nets, even when ReLUs are not used. A possible justification is that constraining the norm of weight vectors allows using big learning rates without the possibility of weights rising in an uncontrolled way [48].



Dropout

A general problem of neural networks is its tendency to overfitting, meaning to learn the particular relationships of training dataset, especially when big architectures are used and training data are limited. Several techniques have been developed for reducing it, including stopping the training as soon as performance on a validation set starts to get worse or introducing weight penalties such as L1 and L2 regularization [49].

Besides, it is known that model combination nearly always improves the performance of machine learning methods. However, training different models and combining their outputs can be computationally expensive both during training and testing time.

Dropout is a technique described in [48] and [50] which is designed to prevent overfitting and to provide a way of combining many different neural network architectures efficiently. The general idea is to “switch off” some randomly selected neurons temporarily, which means that all its incoming and outgoing connections are disconnected (see Figure 19). So on each presentation of each training case, each hidden unit is randomly omitted from the network with a p probability, so that a hidden unit cannot rely on other hidden units being present, preventing the occurrence of complex co-adaptations between neurons. $p = 0.5$ has been demonstrated to produce close to optimal for a wide range of networks and tasks.

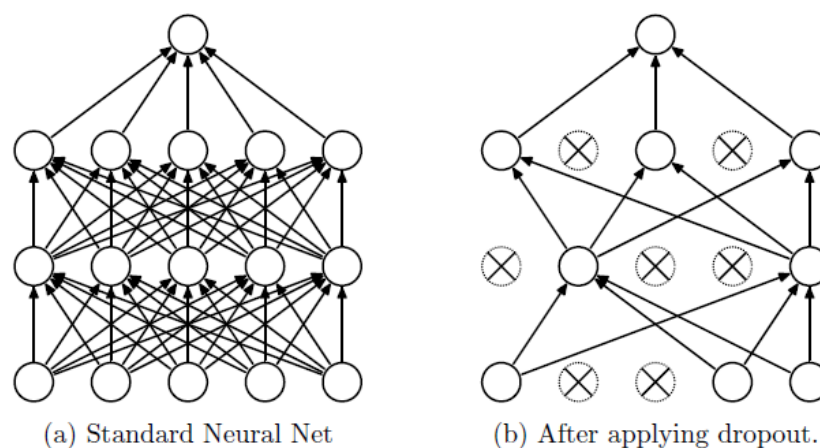


Figure 19. Dropout Neural Net Model. a) Standard neural net with 2 hidden layers. b) Result of applying dropout to the network on the left in a particular iteration of training. Crossed units have been dropped. [48]

That way, training a neural net with n units with dropout can be seen as training a collection of 2^n possible networks with a tiny fraction of the training data where all networks share weights. During test time, an “averaged network” that contains all hidden units activated is employed, but then their outgoing weights must be halved to compensate the fact that all of them are active and not only half of them as during training. This is approximately equivalent to calculate the geometric mean of the probability distributions over labels predicted by all 2^n possible networks.

Dropout introduces a significant amount of noise in the gradients compared to standard stochastic gradient descent. A recommended way to reduce the effect of noise is to use a high momentum, between 0.95 and 0.99 [48]. Momentum of 0.95 has been used in this essay when using dropout.

Toolbox

Deep Learn Toolbox for Matlab, developed by Rasmus Berg Palm for his Master Thesis [51], was used for training and testing the different architectures and techniques explored in this Master Thesis. The toolbox includes logistic and softmax activation, and also options to control dropout fraction and momentum. Learning rate scaling, ReLU activation function and max-norm regularization were implemented to expand the functionality of the toolbox.





5. Experiments

Database

In this essay, MITDB and AFDB have been for training and testing the classification system. As it has been seen in previous section, MITDB is the database considered in the standard *IEC 60601-2-47*, and it was designed to contain a representation of typical cardiac pathologic rhythms and also some infrequent but relevant ones. MITDB has been considered as the client's database, i.e., the database delivered to us by a hypothetical client with the purpose of developing an AF detector.

MITDB was divided into three datasets: test, validation and training sets. As it has been discussed previously, MITDB is formed by 100 and 200 series, and only some records in 200 series contains AF. Sets were generated by randomly selecting a proportional number of records from each series and an amount of records with an approximately duration of AF proportional for each set. The proportion of testing set was a 30% of the MITDB; from the remaining 70% of MITDB, a 30% was selected for validation and a 70% for training sets. Table 3 illustrates the partition.

Table 3. Composition of test, validation and train datasets.

Dataset	MITDB record names	Total Records	Time of AF
Test	103, 108, 109, 114, 119, 121, 202, 205, 219, 220, 228, 232, 233	13	29 min
Validation	106, 112, 122, 123, 201, 203, 215, 230, 231	9	25 min
Train	100, 101, 105, 111, 113, 115, 116, 117, 118, 124, 200, 207, 208, 209, 210, 212, 213, 214, 221, 222, 223, 234,	22	51 min

Testing dataset was used to know the expected error of the classifier when unknown samples are shown to the system. Validation dataset was used to evaluate the training, select optimal parameters and avoid overfitting.

As discussed before, MITDB has scarce samples of AF and a wide sample of confusing rhythms. With the objective of increasing the number of AF samples, the



training dataset was enriched by adding the whole AFDB. The benefits of including AFDB in the training dataset are evaluated in next sections.

As it was disclosed in the development goals, the system should classify segments of 30 seconds of ECG. Thus, each signal was divided into 30-second segments of AF or non-AF rhythm. Segments containing a part of AF and a part of non-AF rhythm were discarded with the aim of letting the classifier to resolve the mixed cases.

Feature Extraction

As it was discussed in chapter 2, several ways of assess RR irregularity have been used in the specific literature. Among all of them, the study of the differences between consecutive RR intervals is a computationally simple and descriptive measure of the irregularity, defined as $\Delta RR_i = RR_{i+1} - RR_i$. In addition to that, the use of RR differences has the advantage of being invariant to heart rate.

Here, Lorentz plot, which is a scatter plot of ΔRR_i vs. ΔRR_{i+1} , have been used to describe the irregularity of RR interval. Each point of a Lorentz plot encodes the uncorrelated nature of three consecutive RR intervals. For example, if three consecutive RR intervals are very similar, the corresponding Lorentz point will be near $(0, 0)$ point. For a short-medium-long sequence, the Lorentz point will be in the first quadrant; long-short-long, in the second quadrant; long-medium-short, in the third quadrant; short-long-short, in the fourth quadrant.

It has been proven that several arrhythmias imprint specific signatures on two dimensional Lorentz plots [52], although the mixture of arrhythmias or some complex ventricular rhythms can generate confusing patterns. In Figure 20 the Lorentz signature of some rhythms is shown.

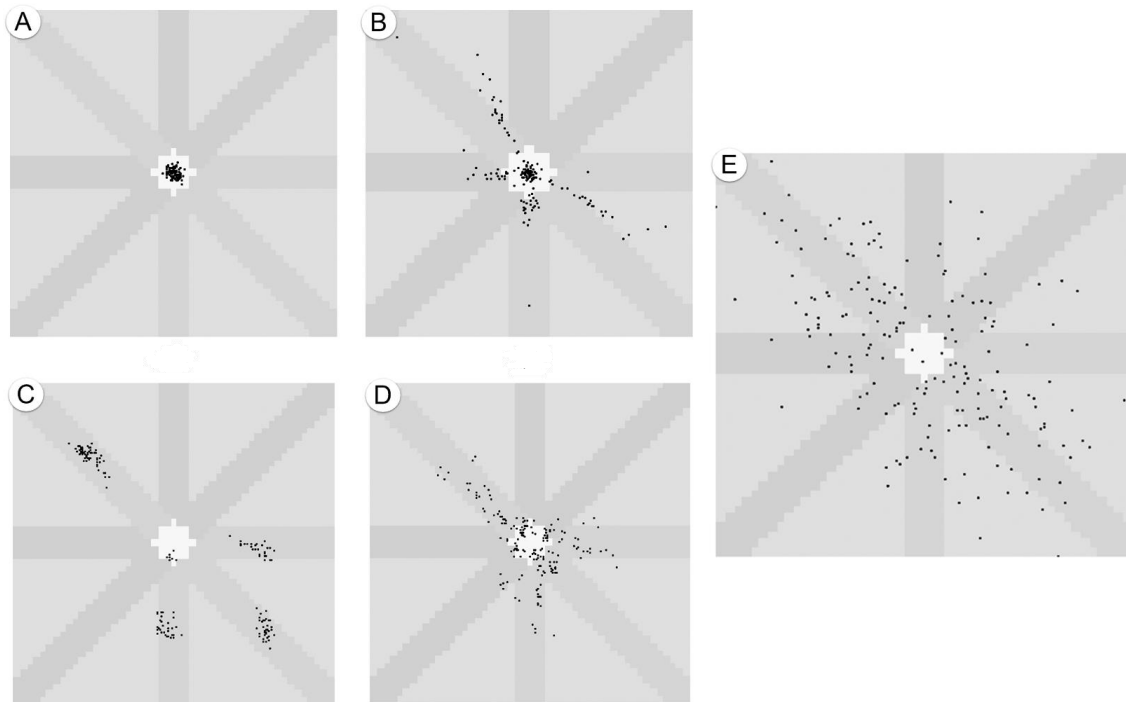


Figure 20. Lorentz plot of different rhythms [32]. A) Normal sinus rhythm. B) Series of premature atrial contractions. C) Atrial tachycardia with grouping beats. D) Atrial tachycardia with irregular ventricular response. E) Atrial fibrillation.

When using neural networks, each instance to be classified must be represented by a feature array of fixed size. 2-dimensional histogram of the Lorentz plot has been used to do so, sampling the Lorentz space from -500 ms to 500 ms in both dimensions. Optimal bin width was a parameter to find.

Developing the Classifier

Common Parameter Tuning

Weights of every configuration were randomly initialized using a constant seed to allow repeatability between experiments.

Architectures of one and two hidden layers have been explored. 2-based logarithmic scale has been used to explore the number of neurons in each layer, with two restrictions: the maximum number of neurons in a layer was the first power of 2 higher than the number of inputs; and the number of neurons of one layer had to be lower or equal to the preceding one. *Softmax* output units were always employed.

Learning rate was selected from a 10-based logarithmic decreasing scale (10^0 , 10^{-1} , 10^{-2} ...). When regular sigmoid-based architectures were used, the selected learning



rate was the highest which allowed quadratic error at training to be monotonically decreasing during first 20 iterations. This is a heuristic that tries to guarantee convergence and fast learning. When ReLU, dropout or max-norm were used, learning rate was ten times lower than the one used in the equivalent sigmoid-based architecture, since was empirically found to converge to good results.

To avoid overfitting on training data, an early stop strategy was followed. For this, classification error at validation dataset was assessed on every epoch during enough epochs to ensure that no more improving on validation set was going to be achieved. Epoch with lowest validation error was selected for each topology.

Defining Histogram Bin Size

Database was characterized by calculating the Lorentz plot histogram of the consecutive RR intervals differences. Several bin sizes were explored with the objective of choosing the one that minimized the number of features (to reduce computational effort) and also minimized the classification error on the validation set. Only datasets generated from MITDB were used at this step.

Bins of 100, 125, 150 and 175 ms were used. They generated feature arrays of 121, 81, 49 and 25 elements, respectively. All possible topologies (with the described restrictions) were used. Topology is indicated using the nomenclature [*input hidden output*], where *input* and *output* are scalars indicating the number of inputs and outputs and *hidden* is an array that refers to the number of neurons in the hidden layers. As ANN with one or two hidden layers are employed, *hidden* can have one or two elements. Validation error was calculated and smaller error for each bin size was selected. When two topologies had the same error, the most compact was selected.

In Annex A, Table 10 to Table 13 show the validation error obtained with different topologies of 1 and 2 layers for features obtained using a bin size of 100, 125, 150 and 175 ms. Table 4 shows a summary of those tables. Minimum validation error of each bin size and the corresponding topology are presented. As it is shown, the bin size of 150 ms is the one that better reflects the complexity of the Lorentz plot for this problem, since it is able to obtain the minimum error. Thus, bin size of 150 ms is selected to generate the features for the classification system.

Table 4. Summary of minimum validation error of each bin size.

Bin Size	Best Topology	Minimum Validation Error
100 ms	[121 128 128 2]	7.54
125 ms	[81 4 4 2]	7.68
<u>150 ms</u>	<u>[49 4 2 2]</u>	<u>6.35</u>
175 ms	[25 16 2 2]	6.81

Adding AFDB to the training dataset

As already discussed in previous sections, MITDB contains reduced samples of AF and also an important variety of complex ventricular and supraventricular rhythms that can be confused with AF. This is why the minimum valid error in the previous section was 6.35%, which is too high for the application.

In this section, AFDB is added to the training dataset to increase the AF samples in order to enable the system to improve the classification between AF and other non AF rhythms. As determined before, bin size of 150 ms is used to generate the features.

All possible topologies were explored: validation errors of all of them are shown in Annex B, Table 14. As it can be seen, adding AFDB to the training dataset allows a general reduction of the validation error. Best result was obtained by using a [49 64 2 2] topology, which obtained a validation error of 5.17%, which means a reduction of the error in a percentage of 19% compared to previous result.

ANN with Dropout

In this section, results of using networks with dropout to improve the performance are shown. All possible architectures were explored. The validation errors are shown in Annex C, Table 15. The best result is obtained by a [49 64 2 2] architecture, that achieves 4.11% of error. This means a 21% reduction of the error obtained in the previous step, verifying that introducing dropout improves the performance, as was demonstrated in [48].



ANN with Dropout and ReLU

Using the best architecture of the previous section, the network was modified to use ReLU in hidden layers and training was performed again. No regularization was introduced in this step. This configuration obtained a validation error of 4.75%, which was worse than the one without ReLU. This is because ReLU propagates big gradients and weights can reach huge values in an uncontrolled way, converging to a sub-optimal solution. In this case, max-norm regularization should be used.

Apply max-norm regularization

In order to control the norm of weight vectors of the ReLU configurations, max-norm regularization was used. 2, 3 and 4 were used as max-norm coefficients, and validation error was calculated this way. Results are shown in Table 5.

Table 5. Validation error of networks using dropout and ReLU and different max-norm coefficients.

Max-norm coefficient	Topology	Validation Error (%)
2	[49 64 2 2]	4.65
3	[49 64 2 2]	3.47
4	[49 64 2 2]	3.45

As it can be seen, the best validation error is obtained using a max-norm regularization coefficient of 4. This configuration achieves a validation error of 3.45%, which means a 16% reduction of the error obtained using only dropout, and also a 27% reduction of the error obtained using dropout and ReLU without regularization.

Conclusion

Several strategies have been implemented to improve the performance of a classifier based on ANN. First strategy was to enrich the training dataset with more samples to represent the classes in a better way, obtaining a reduction of 19% in the validation error. Secondly, dropout was used, and error was reduced a 21% more. Third, ReLU was used and, if no regularization was used, the error became worse. However, if max-norm regularization with a coefficient of 4 was used, the error was reduced again by 16%. Results are shown in Table 6. Summing up, from the first to the last step, the error was reduced by a 45%.

Table 6. Evolution of validation error using different strategies to improve learning.

Strategy	Topology	Validation Error (%)
Plain ANN	[49 4 2 2]	6.35
+ AFDB to training set	[49 64 2 2]	5.17
+ Dropout	[49 64 2 2]	4.11
+ ReLU	[49 64 2 2]	4.75
+ Max-norm (4)	[49 64 2 2]	3.45

Hold Out: Results on Test Dataset

In the previous section, it has been demonstrated that the best way to model our problem employing ANN is: to use a histogram bin of 150 ms (thus using 49-element features); to include AFDB in the training set; and to use an architecture of two hidden layers with 64 and 2 neurons respectively, employing dropout, ReLU and max-norm regularization, with 4 as regularization coefficient.

In this section, the results of the developed system on test dataset are presented. For this, the hyper-parameters obtained in the previous section (learning rate, epochs, architecture, etc.) were used to train an ANN using training and validation datasets. Results on test database are shown in Table 7. As it can be seen, test error is lower than validation error. A possible explanation for this is that validation dataset contains important information not included in the training dataset that helps to improve the classification on test dataset. In addition to classification error, sensitivity, specificity and positive predictivity were calculated.

Table 7. Hold out: results on test dataset of the developed system.

Error (%)	Sensitivity (%)	Specificity (%)	Positive Predictivity (%)
2.13	91.02	98.52	85.31

The results on test dataset reflect the behavior of the system when completely new signals are analyzed in the future. As seen in Table 7, sensitivity and positive predictivity overcome the objectives proposed for this Master Thesis.





6. Commercial Product Development

Prototype

This AF classifier has been developed to be integrated in an ECG analysis system that requires the capability of detecting AF events. Before the integration, the system is trained with all available data, including AFDB and MITDB. The obtained ANN is a prototype of AF classifier that could be integrated in different ECG analysis algorithms, such as embedded systems in implantable or external cardiac monitors, or offline analysis platforms as holter analysis software. The performance on MITDB of this prototype is disclosed in Table 8.

Table 8. Results on MITDB of the prototype of AF classifier.

Error (%)	Sensitivity (%)	Specificity (%)	Positive Predictivity (%)
1.48	94.50	97.92	89.80

Integration

The prototype developed in the previous section has been integrated in *nECG Suite*, the software to analyze long-term holter recordings developed by Nuubo. Nuubo has designed and implemented its own ECG processing algorithms including QRS detection, QRS morphologic clustering, beat classification and arrhythmia detection.

All ANN utilities needed for the integration were implemented and included in *nECG Suite*. Beat detections generated by *nECG Suite* were used as input to the integrated AF classifier. Also, the test environment described in *IEC 60601-2-47* to assess the performance of the classifier was developed. For that purpose, some utilities suggested by the standard and available in www.physionet.org were used:

- **xform**: generates a new signal file and annotation file with different sampling frequency, amplitude and also a portion of the record can be copied. This was used to resample the signal, since MITDB is sampled at 360 Hz and *nECG Suite* is tuned to work with a sampling frequency of 250 Hz. Complete signals and their original amplitudes were used.



- **epicmp**: implements the VF, AF, and ST episode-by-episode comparison algorithms specified by the current American National Standard for ambulatory ECG analyzers (*ANSI/AAMI EC38:2007*, which is the implementation in the US of *IEC 60601-2-47*).

Also, WFDB C# Wrapper, developed by Boutemine Oualid [53], was used to read signals and write annotations in the format specified in *WFDB Programmer's Guide* [54].

The result of the AF performance assessment based on duration of the episodes as indicated in *IEC 60601-2-47* is disclosed in Table 9. As it can be appreciated, *nECG Suite* reaches a sensitivity of 93% and a positive predictivity of 87%, which is slightly lower than the statistics of the prototype shown in Table 8. This small reduction could be explained because of the differences in the position of the analysis window used by the classifier.

In order to allow comparisons, SEEQ statistics are also disclosed in Table 9. SEEQ shows a sensitivity of 90% and positive predictivity of 85%. Therefore, the developed AF classifier integrated in *nECG Suite* overcomes the performance of SEEQ, which was one of the proposed objectives of this Master Thesis, together with the use of the information contained in the inter-beat interval sequence of a 30 second segment to perform the classification.

Table 9. AF performance on MITDB (duration measurement as disclosed on *IEC 60601-2-47*) of the developed prototype integrated in *nECG Suite* by Nuubo, compared with SEEQ (Medtronic).

	Sensitivity (%)	Positive Predictivity (%)
<i>nECG Suite</i>	93	87
SEEQ	90	85

7. Conclusions

The main goal of this Master Thesis was to develop a classifier able to distinguish between atrial fibrillation (AF) and non-AF rhythms using the information contained in the inter-beat interval sequence of a segment of 30 seconds. Thus, every detected beat is considered and no morphology assessment is needed in order to eliminate ectopic beats that can be confused with AF rhythm. This way, the classifier could be integrated in any ECG analysis system that performs beat detection, such as implantable or external cardiac monitors or offline analysis platforms as holter analysis software.

In the first section, heart physiology and AF mechanisms and symptoms have been discussed. AF is the most common sustained arrhythmia, affecting 1–2% of the population. It is a fast arrhythmia characterized by the set up of recurrent, multiple and uncoordinated electrical waves in the atrium that excite the atrial myocardium in a totally disorganized way. As a result, atrial contraction is inexistent and ventricular beats are fast and arrhythmic. AF is associated with a 5-fold risk of stroke and an augmented morbi-mortality of patients with AF. Also, those patients suffer from palpitations, fatigue, faintness or shortness of breath, among other symptoms, which considerably reduce their quality of life and their exercise capacity.

In the second section, several strategies to monitor the ECG ambulatorily were analyzed, going from the traditional holter test to more innovative techniques focused on long-term monitoring, as adhesive patches, textile holter or implantable cardiac monitors. Together with this, a review of the state of the art in AF detection was performed, considering both academic solutions and industrial solutions. Among the industrial solutions, SEEQ (by Medtronic) is, to our concern, the only one which publishes its AF detection statistics on public standard databases (MIT-BIH Arrhythmia Database), achieving a sensitivity of 90% and a positive predictivity of 85%. To overcome these statistics was an objective of this Master Thesis.

Artificial neural networks (ANN) were the chosen tool to achieve the proposed objective. In the fourth section a brief description of ANN has been performed. And also, several techniques to improve their learning capabilities have been discussed, such as employing rectified linear units (ReLU) in the hidden layers or dropout



mechanism, which temporally disables random neurons during training time to improve generalization.

Using public annotated database from Physionet (MIT-BIH Arrhythmia Database and MIT-BIH Atrial Fibrillation Database), and following a hold out strategy, three dataset were made, one to train, another to validate the results of the training and a third one to test the final performance. Besides, best features to describe the problem were determined by using plain ANN. Then, the mentioned techniques to improve learning capabilities were explored in an incremental approach, verifying that each new technique reduced the classification error on the validation dataset.

The result of this optimization process was a reduction of classification error in a 45%. The best network had two hidden layers of 64 and 2 neurons respectively and implemented dropout, *softmax* output units, ReLU in hidden layers and max-norm regularization. On test dataset, classification error was 2.13%, sensitivity 91.02%, specificity 98.52% and positive predictivity 85.31%. So the behavior of this classifier when completely new signals are analyzed overcomes the proposed objective.

This classification system was prototyped to be introduced in an ECG analysis system that requires the capability of detecting AF events. To do this, a system with the hyper-parameters obtained in the develop stage was trained using all available data, i.e., training, validation and test datasets. This prototype had a classification error on MIT-BIH Arrhythmia Database of 1.48%, a sensitivity of 94.50%, a specificity of 97.92% and a positive predictivity of 89.80%.

Finally, the prototype was integrated in a software solution to analyze long-term holter recordings developed by Nuubo, called *nECG Suite*. This software uses proprietary algorithms to perform QRS detection, QRS morphology clustering, beat classification and arrhythmia detection. Also, the test environment described in *IEC 60601-2-47* to assess the performance of the classifier was developed. The evaluation shows that *nECG Suite* has a sensitivity of 93% and a positive predictivity of 87%, overcoming the proposed objective of 90% and 85% respectively fulfilling the requirement of only using the inter-beat interval sequence contained in 30-second segments.

8. References

- [1] Guyton AC, Hall JE. *Textbook of Medical Physiology*, 11 ed Elsevier Saunders, 2006.
- [2] Berret K, Brooks H, Boitano S, Barman S. *Ganong's Review of Medical Physiology*, 23 ed. Mc Graw Hill Medical, 2010.
- [3] Runge MS, Stouffer G, Patterson C. *Netter's Cardiology*. Elsevier Health Sciences. 2010
- [4] Camm AJ, Kirchhof P, Lip GY, et al. Guidelines for the management of atrial fibrillation. *European heart journal*, 2010, v.31, pp.2369–2429.
- [5] January CT, Wann LS, Alpert JS, et al. AHA/ACC/HRS guideline for the management of patients with atrial fibrillation: a report of the American College of Cardiology/American Heart Association Task Force on Practice Guidelines and the Heart Rhythm Society. *Journal of the American College of Cardiology*, 2014, v.64(21), pp.2246–2280.
- [6] Charitos EI, Stierle U, Ziegler PD, et al. A Comprehensive Evaluation of Rhythm Monitoring Strategies for the Detection of Atrial Fibrillation Recurrence Insights From 647 Continuously Monitored Patients and Implications for Monitoring After Therapeutic Interventions. *Circulation*, 2012, v.126(7), pp.806–814.
- [7] Kirchhof P, Auricchio A, Bax J, et al. Outcome parameters for trials in atrial fibrillation: executive summary. Recommendations from a consensus conference organized by the German Atrial Fibrillation Competence NETwork (AFNET) and the European Heart Rhythm Association (EHRA). *European heart journal*, 2007, v.28, pp.2803–2817.
- [8] Zimetbaum P, Goldman A, Ambulatory Arrhythmia Monitoring Choosing the Right Device. *Circulation*, 2010, v.122(16), pp.1629–1636.
- [9] Crawford MH, Bernstein SJ, Deedwania PC, et al., ACC/AHA guidelines for ambulatory electrocardiography: executive summary and recommendations a report of the American College of Cardiology/American Heart Association Task Force on Practice Guidelines (Committee to Revise the Guidelines for Ambulatory Electrocardiography) developed in collaboration with the North American Society for Pacing and Electrophysiology. *Circulation*, 1999, v.100(8), pp.886-893.
- [10] Barrett PM, Komatireddy R, Haaser S, et al., Comparison of 24-hour Holter monitoring with 14-day novel adhesive patch electrocardiographic monitoring. *The American journal of medicine*, 2014, v.127(1), pp.95.e11-e17.
- [11] Turakhia MP, Hoang DD, Zimetbaum P, et al., Diagnostic utility of a novel leadless arrhythmia monitoring device. *The American journal of cardiology*, 2013, v.112(4), pp.520-524.
- [12] Lobodzinski SS, ECG patch monitors for assessment of cardiac rhythm abnormalities. *Progress in cardiovascular diseases*, 2013, v.56(2), pp.224-229.
- [13] Olmos C, Franco E, Suárez-Barrientos A, et al., Wearable wireless remote monitoring system: An alternative for prolonged electrocardiographic monitoring. *International journal of cardiology*, 2014, v.1(172), pp.e43-e44.
- [14] Perez de Isla L, Lennie V, Quezada M, et al., New generation dynamic, wireless and remote cardiac monitorization platform: a feasibility study. *International journal of cardiology*, 2011, v.153(1), pp.83-85.



- [15] Fabregat-Andres O, Munoz-Macho A, Adell-Beltran G, Ibanez-Catala X, et al, Evaluation of a New Shirt-Based Electrocardiogram Device for Cardiac Screening in Soccer Players: Comparative Study With Treadmill Ergospirometry. *Cardiology Research*, 2014, v.5(3-4), pp.101-107.
- [16] Fabregat-Andrés O, Muñoz-Macho A, Adell-Beltrá G, Fácila, L, Feasibility of using a new generation wireless device for electrocardiographic monitoring of professional soccer players during an exercise test in field: a pilot study. *The Journal of sports medicine and physical fitness*. 2014.
- [17] <http://www.cms.gov/>
- [18] Tompkins J, Pan W, A real-time QRS detection algorithm. *IEEE Transactions on Biomedical Engineering*, 1985, v.32, pp.230-236.
- [19] Köhler BU, Hennig C, Orglmeister R, The principles of software QRS detection. *Engineering in Medicine and Biology Magazine, IEEE*, 2002, v.21(1), pp.42-57.
- [20] Pürerfellner H, Pokushalov E, Sarkar S, et al., P-wave evidence as a method for improving algorithm to detect atrial fibrillation in insertable cardiac monitors. *Heart Rhythm*, 2014, v.11(9), pp.1575-1583.
- [21] Cubanski D, Cyganski D, Antman E M, Feldman, CL, A neural network system for detection of atrial fibrillation in ambulatory electrocardiograms. *Journal of cardiovascular electrophysiology*, 1994, v.5(7), pp.602-608.
- [22] Hindricks G, Pokushalov E, Urban L, et al., Performance of a new leadless implantable cardiac monitor in detecting and quantifying atrial fibrillation results of the XPECT trial. *Circulation: Arrhythmia and Electrophysiology*, 2010, v.3(2), pp.141-147.
- [23] Goldberger AL, Amaral LAN, Glass L, et al. PhysioBank, PhysioToolkit, and PhysioNet: Components of a New Research Resource for Complex Physiologic Signals. *Circulation*, 2000, v.101(23), pp.e215-e220
- [24] <http://www.physionet.org/physiobank/database/html/mitdbdir/mitdbdir.htm>
- [25] Moody GB, Mark RG. A new method for detecting atrial fibrillation using R-R intervals. *Computers in Cardiology*, 1983, pp.227-230.
- [26] Artis SG, Mark RG, Moody, GB, Detection of atrial fibrillation using artificial neural networks. *Computers in Cardiology*, 1991, pp.173-176
- [27] Young B, Brodnick D, Spaulding R, A comparative study of a hidden Markov model detector for atrial fibrillation. *Neural Networks for Signal Processing IX*, 1999, pp. 468-476.
- [28] Tateno K, Glass L, A method for detection of atrial fibrillation using RR intervals. *Computers in Cardiology*, 2000, pp.391-394.
- [29] Tateno K, Glass L, Automatic detection of atrial fibrillation using the coefficient of variation and density histograms of RR and Δ RR intervals. *Medical and Biological Engineering and Computing*, 2001, v.39(6), pp.664-671.
- [30] Ghodrati A, Marinello S, Statistical analysis of RR interval irregularities for detection of atrial fibrillation. *Computers in Cardiology*, 2008, pp.1057-1060.
- [31] Couceiro R, Carvalho P, Henriques J, et al., Detection of atrial fibrillation using model-based ECG analysis, *19th International Conference on Pattern Recognition*, 2008, pp.1-5.
- [32] Sarkar S, Ritscher D, Mehra R, A detector for a chronic implantable atrial tachyarrhythmia monitor, *IEEE Transactions on Biomedical Engineering*, 2008, v.55(3), pp.1219-1224.
- [33] Dash S, Chon KH, Lu S, Raeder EA, Automatic real time detection of atrial fibrillation. *Annals of biomedical engineering*, 2009, v.37(9), pp.1701-1709.

- [34] Babaeizadeh S, Gregg RE, Helfenbein ED, et al., Improvements in atrial fibrillation detection for real-time monitoring. *Journal of electrocardiology*, 2009, v.42(6), pp.522-526.
- [35] Huang C, Ye S, Chen H, et al., A novel method for detection of the transition between atrial fibrillation and sinus rhythm. *IEEE Transactions on Biomedical Engineering*, 2011, v.58(4), pp.1113-1119.
- [36] Lian J, Wang L, Muessig D, A simple method to detect atrial fibrillation using RR intervals. *The American journal of cardiology*, 2011, v.107(10), pp.1494-1497.
- [37] Zhou X, Ding H, Ung B, et al, Automatic online detection of atrial fibrillation based on symbolic dynamics and Shannon entropy. *Biomedical engineering online*, 2014, v.13(1), p.18.
- [38] Petrénas A, Marozas V, Sörnmo L. Low-complexity detection of atrial fibrillation in continuous long-term monitoring. *Computers in biology and medicine*, 2015, <http://dx.doi.org/10.1016/j.compbio.2015.01.019>
- [39] IEC 60601-2-47:2012 – Medical electrical equipment – Part 2-47: Particular requirements for the basic safety and essential performance of ambulatory electrocardiographic systems.
- [40] Rosenblatt F. The Perceptron—a Perceiving and Recognizing Automation. *Technical Report 85-460-1*. 1957. Cornell Aeronautical Laboratory, Ithaca.
- [41] Hu YH, Hwang JN, (Eds.). *Handbook of neural network signal processing*. CRC press. 2001.
- [42] McCulloch WS, Pitts W. A logical calculus of the ideas immanent in nervous activity. *The bulletin of mathematical biophysics*, 1943, v.5(4), pp.115-133.
- [43] Cybenko G. Approximation by superpositions of a sigmoidal function. *Mathematics of control, signals and systems*, 1989, v.2(4), pp.303-314.
- [44] Rumelhart DE, McClelland JL (Eds.). *The PDP Research Group: Parallel distributed processing: Explorations in the microstructure of cognition. Volume 1; Foundations*. MIT Press, 1986.
- [45] Bishop, Christopher. *Neural networks for pattern recognition*. Clarendon Press, 1995.
- [46] LeCun YA, Bottou L, Orr GB, et al, Efficient backprop. *Neural networks: Tricks of the trade*, 2012, pp. 9-48.
- [47] Zeiler MD, Ranzato MA, Monga R, et al. On rectified linear units for speech processing. *IEEE International Conference on Acoustics, Speech and Signal Processing (ICASSP)*, 2013. pp. 3517-3521.
- [48] Srivastava N, Hinton G, Krizhevsky A, et al. Dropout: A simple way to prevent neural networks from overfitting. *The Journal of Machine Learning Research*, 2014, v.15(1), pp.1929-1958.
- [49] Ng AY. Feature selection, L1 vs. L2 regularization, and rotational invariance. In *Proceedings of the twenty-first international conference on Machine learning*. 2004. p. 78.
- [50] Hinton GE, Srivastava N, Krizhevsky A, et al. Improving neural networks by preventing co-adaptation of feature detectors. 2012, *arXiv preprint arXiv:1207.0580*.
- [51] Palm RB. Prediction as a candidate for learning deep hierarchical models of data. *Technical University of Denmark*. 2012.
- [52] Esperer HD, Esperer C, Cohen RJ. Cardiac arrhythmias imprint specific signatures on Lorenz plots. *Annals of Noninvasive Electrocardiology*, 2008, v.13(1), pp.44-60.
- [53] <https://github.com/BoutemineOualid/WfdbCsharpWrapper>
- [54] <http://www.physionet.org/physiotools/wpg/>





A. Annex: Bin size exploration

Table 10. Validation error of different topologies of 1 and 2 layers using a bin size of 100 ms. Best result is underlined and bold.

Bin Size: 100ms		
	Topology	Validation Error (%)
1 Layer	[121 2 2]	9.99
	[121 4 2]	9.32
	[121 8 2]	7.95
	[121 16 2]	9.20
	[121 32 2]	8.76
	[121 64 2]	8.76
	[121 128 2]	7.95
2 Layers	[121 2 2 2]	10.30
	[121 4 2 2]	9.63
	[121 4 4 2]	9.28
	[121 8 2 2]	8.30
	[121 8 4 2]	9.16
	[121 8 8 2]	8.91
	[121 16 2 2]	8.20
	[121 16 4 2]	8.49
	[121 16 8 2]	8.84
	[121 16 16 2]	8.03
	[121 32 2 2]	8.93
	[121 32 4 2]	8.99
	[121 32 8 2]	8.53
	[121 32 16 2]	8.35
	[121 32 32 2]	8.72
	[121 64 2 2]	8.14
	[121 64 4 2]	8.12
	[121 64 8 2]	8.45
	[121 64 16 2]	8.32
	[121 64 32 2]	8.24
	[121 64 64 2]	8.37
	[121 128 2 2]	8.16
	[121 128 4 2]	7.93
	[121 128 8 2]	7.66
	[121 128 16 2]	8.03
	[121 128 32 2]	7.99
	[121 128 64 2]	8.64
	<u>[121 128 128 2]</u>	<u>7.54</u>



Table 11. Validation error of different topologies of 1 and 2 layers using a bin size of 125 ms. Best results are underlined and bold.

Bin Size: 125ms		
	Topology	Validation Error (%)
1 Layer	[81 2 2]	10.50
	[81 4 2]	8.68
	[81 8 2]	9.99
	[81 16 2]	9.92
	[81 32 2]	9.05
	[81 64 2]	8.37
	[81 128 2]	8.49
2 Layers	[81 2 2 2]	9.40
	[81 4 2 2]	8.32
	[81 4 4 2]	7.68
	[81 8 2 2]	8.03
	[81 8 4 2]	9.22
	[81 8 8 2]	10.36
	[81 16 2 2]	9.18
	[81 16 4 2]	8.30
	[81 16 8 2]	9.32
	[81 16 16 2]	9.11
	[81 32 2 2]	10.26
	[81 32 4 2]	9.59
	[81 32 8 2]	9.51
	[81 32 16 2]	8.78
	[81 32 32 2]	9.03
	[81 64 2 2]	9.03
	[81 64 4 2]	8.93
	[81 64 8 2]	8.43
	[81 64 16 2]	8.80
	[81 64 32 2]	8.66
	[81 64 64 2]	8.76
	[81 128 2 2]	8.74
	[81 128 4 2]	7.91
	[81 128 8 2]	8.59
	[81 128 16 2]	8.91
	[81 128 32 2]	8.49
	[81 128 64 2]	7.68
[81 128 128 2]	8.30	

Table 12. Validation error of different topologies of 1 and 2 layers using a bin size of 150 ms. Best result is underlined and bold.

Bin Size: 150ms		
	Topology	Validation Error (%)
1 Layer	[49 2 2]	8.57
	[49 4 2]	9.32
	[49 8 2]	7.66
	[49 16 2]	8.62
	[49 32 2]	8.78
	[49 64 2]	7.54
2 Layers	[49 2 2 2]	8.26
	<u>[49 4 2 2]</u>	<u>6.35</u>
	[49 4 4 2]	8.57
	[49 8 2 2]	8.37
	[49 8 4 2]	8.24
	[49 8 8 2]	7.52
	[49 16 2 2]	7.99
	[49 16 4 2]	8.78
	[49 16 8 2]	7.85
	[49 16 16 2]	8.76
	[49 32 2 2]	8.84
	[49 32 4 2]	7.54
	[49 32 8 2]	8.12
	[49 32 16 2]	7.54
	[49 32 32 2]	8.05
	[49 64 2 2]	7.35
	[49 64 4 2]	6.79
	[49 64 8 2]	7.56
	[49 64 16 2]	7.74
	[49 64 32 2]	8.24
[49 64 64 2]	7.93	



Table 13. Validation error of different topologies of 1 and 2 layers using a bin size of 175 ms. Best result is underlined and bold.

Bin Size: 175ms		
	Topology	Validation Error (%)
1 Layer	[25 2 2]	8.64
	[25 4 2]	8.59
	[25 8 2]	9.26
	[25 16 2]	8.01
	[25 32 2]	9.38
2 Layers	[25 2 2 2]	7.91
	[25 4 2 2]	9.45
	[25 4 4 2]	9.65
	[25 8 2 2]	8.59
	[25 8 4 2]	7.93
	[25 8 8 2]	7.83
	<u>[25 16 2 2]</u>	<u>6.81</u>
	[25 16 4 2]	9.24
	[25 16 8 2]	7.47
	[25 16 16 2]	7.37
	[25 32 2 2]	8.10
	[25 32 4 2]	7.64
	[25 32 8 2]	8.64
	[25 32 16 2]	8.59
[25 32 32 2]	7.54	

B. Annex: Training with AFDB

Table 14. Validation error of different topologies of 1 and 2 layers using a bin size of 150 ms and including AFDB in the training dataset. Best result is underlined and bold.

	Topology	Validation Error (%)
1 Layer	[49 2 2]	7.08
	[49 4 2]	6.83
	[49 8 2]	5.56
	[49 16 2]	6.04
	[49 32 2]	6.31
	[49 64 2]	6.44
2 Layers	[49 2 2 2]	7.99
	[49 4 2 2]	6.06
	[49 4 4 2]	6.68
	[49 8 2 2]	5.88
	[49 8 4 2]	6.58
	[49 8 8 2]	6.35
	[49 16 2 2]	5.81
	[49 16 4 2]	6.79
	[49 16 8 2]	6.27
	[49 16 16 2]	6.27
	[49 32 2 2]	6.27
	[49 32 4 2]	6.19
	[49 32 8 2]	6.56
	[49 32 16 2]	6.54
	[49 32 32 2]	5.65
	<u>[49 64 2 2]</u>	<u>5.17</u>
	[49 64 4 2]	6.08
	[49 64 8 2]	5.19
	[49 64 16 2]	5.92
	[49 64 32 2]	5.27
[49 64 64 2]	5.79	





C. Annex: ANN with Dropout

Table 15. Validation error of different topologies of 1 and 2 layers using dropout networks. Best result is underlined and bold.

	Topology	Validation Error (%)
1 Layer	[49 2 2]	5.71
	[49 4 2]	8.10
	[49 8 2]	8.32
	[49 16 2]	6.95
	[49 32 2]	6.64
	[49 64 2]	5.23
2 Layers	[49 2 2 2]	11.87
	[49 4 2 2]	5.31
	[49 4 4 2]	9.05
	[49 8 2 2]	6.23
	[49 8 4 2]	6.60
	[49 8 8 2]	8.43
	[49 16 2 2]	5.63
	[49 16 4 2]	9.13
	[49 16 8 2]	6.02
	[49 16 16 2]	9.09
	[49 32 2 2]	5.07
	[49 32 4 2]	6.56
	[49 32 8 2]	7.97
	[49 32 16 2]	6.73
	[49 32 32 2]	6.95
	<u>[49 64 2 2]</u>	<u>4.11</u>
	[49 64 4 2]	4.36
	[49 64 8 2]	4.50
	[49 64 16 2]	4.59
	[49 64 32 2]	5.29
[49 64 64 2]	5.23	

